Journal of Engineering
SPECIAL ISSUE Sustainable Engineering Practices

WILEY

RESEARCH ARTICLE OPEN ACCESS

Synergistic Effects of Jatropha Biodiesel and TiO_2 Nanoparticles on the Performance and Emission Characteristics of a Diesel Engine

Muhammad Sarfraz Ali[1,2] | Asad Naeem Shah[2] | Laurencas Raslavičius[1] | Sadia Saleem[3] | Shanawar Hamid[4] | Eustache Hakizimana[5]

[1]Department of Transport Engineering, Faculty of Mechanical Engineering and Design, Kaunas University of Technology, Kaunas, LT-51424, Lithuania | [2]Department of Mechanical Engineering, University of Engineering and Technology, Lahore 54890, Pakistan | [3]Institute of CS and IT, The Women University, Multan 60000, Pakistan | [4]Advanced Integrated Energy Lab, Department of Sciences, School of Interdisciplinary Sciences and Engineering, National University of Sciences and Technology (NUST), H-12, Islamabad 44000, Pakistan | [5]Department of Mechanical and Energy Engineering, University of Rwanda, Kigali, Rwanda

Correspondence: Muhammad Sarfraz Ali (engrmsa1@gmail.com) | Eustache Hakizimana (haki2012eustache@gmail.com)

Received: 18 August 2025 | **Revised:** 8 March 2026 | **Accepted:** 25 March 2026

Guest Editor: Arnab Biswas

Keywords: diesel engine | emissions | engine performance | fuel additives | Jatropha biodiesel | titanium dioxide nanoparticles

ABSTRACT

The performance and emission characteristics of a water-cooled, four-stroke, three-cylinder compression ignition (CI) engine were examined in this work in relation to the synergetic effects of titanium dioxide (TiO_2) nanoparticles and Jatropha methyl ester (JME) biodiesel. A variety of fuel blends, including B10 and B20 (10% and 20% JME by volume), as well as their corresponding nanoparticle-enhanced versions (B10T30, B10T60, B10T90, B20T30, B20T60, and B20T90), were used in the experimental testing. Pure diesel (D) was used as the baseline. In order to assess important performance parameters, including torque, brake-specific fuel consumption (BSFC), brake thermal efficiency (BTE), and emission parameters like nitrogen oxide (NO_x), hydrocarbons (HC), carbon monoxide (CO), and smoke opacity, the engine was operated under constant full load conditions, with the speed adjusted between 1200 and 2200 rpm in increments of 200 rpm. The findings show that adding TiO_2 nanoparticles greatly enhances engine performance. When compared to diesel, the B20T90 and B10T90 showed the most substantial gains, with BTE increases of up to 6.2% and BSFC reductions of 3.4%. All TiO_2-enhanced blends showed much lower CO and smoke emissions, suggesting cleaner burning though HC emissions increased at higher nanoparticle concentrations, possibly due to agglomeration effects. However, because of excessive oxygen availability and higher combustion temperature, there was an increase in HC and NO_x emissions. Overall, the results show that JME and TiO_2 work in combination to improve fuel economy and lower particle emissions. If the issue of cost-effective nanoparticle sourcing is resolved, these fuel blends—in particular, B10T90 and B20T90—show potential for short-term benefits in controlled laboratory conditions, but substantial further work is required on long-term durability, regulatory pathways, and cost-benefit ratios compared to existing aftertreatment systems such as SCR and DPF, to assess their viability for sustainable diesel engine operation in the industrial and transportation sectors.

Muhammad Sarfraz Ali and Sadia Saleem are contributed equally to this work and should be listed as co-first author.

1 | Introduction

Diesel engines have long been preferred in the fields of power generation, transportation, and agriculture because of their exceptional torque, durability, and fuel efficiency [1]. However, because of the type and amount of emissions they create, their extensive use has sparked serious environmental concerns. In contrast to petrol engines, diesel engines run at higher compression ratios and lean burn circumstances, which can result in the production of complex pollutants that are extremely dangerous for human health and the environment [2].

Nitrogen oxide (NO_x) emissions from diesel engines are one of the main environmental issues. These chemicals are important precursors of acid rain and help create smog and ground-level ozone. Emissions of NO_x have been classified as harmful air pollutants and are linked to respiratory conditions [3]. Additionally, diesel engines emit particulate matter (PM), particularly fine particles ($PM_{2.5}$), which can penetrate the bloodstream and penetrate deep into the lungs, resulting in cardiovascular and pulmonary diseases [4]. Other harmful emissions from diesel engines include carbon monoxide (CO), unburned hydrocarbons (HC), and sulfur oxides (SO_x). Both CO and HC are byproducts of incomplete combustion that contribute to air pollution and directly threaten human health [5]. Even if advancements in fuel formulations and after-treatment systems have reduced emissions to some extent, diesel exhaust remains a significant cause of urban air pollution. This is especially true in developing countries where regular usage of emission control systems is lacking.

Usually made by the transesterification method, biodiesel is a mono-alkyl ester of long-chain fatty acids obtained from renewable lipid sources like vegetable or animal fat [6, 7]. It can be mixed with regular diesel in different ratios (e.g., B10, B20) or utilized in its pure form (B100). Because biodiesel shares characteristics with petroleum diesel, it can be used in diesel engines that are already in use without requiring significant changes [8]. The non-edible oil-bearing plant *Jatropha curcas* has garnered a lot of interest among feedstocks for the creation of biodiesel. Jatropha is a drought-tolerant, robust plant that requires little agricultural input to grow on marginal soil [9]. Because it doesn't directly compete with food crops, it is particularly well-suited for nations with a shortage of arable land and worries about food security. The Jatropha methyl ester (JME), which is derived from Jatropha oil, has favorable physicochemical characteristics that make it safer to handle and store than regular diesel [10]. These include a high cetane number, good lubrication, and a substantially higher flash point.

The use of biodiesel blended with metallic nanoparticles as a fuel additive in diesel engines has emerged as a promising approach to enhance performance and reduce emissions [11]. Biodiesel improves combustion due to its oxygen content but often leads to higher NO_x emissions. Adding metallic nanoparticles such as Al_2O_3, TiO_2, CuO, CeO_2, and ZnO enhances combustion efficiency by acting as catalysts, potentially improving atomization at optimal concentrations, and promoting complete fuel oxidation [12]. Research shows that biodiesel-nanoparticle blends increase brake thermal efficiency (BTE), lower fuel consumption, and significantly reduce CO, HC, and smoke emissions [13]. Moreover, the rise in NO_x emissions associated with biodiesel can be controlled by optimizing nanoparticle concentration or using EGR. The synergistic effect of nanoparticles improves heat transfer and combustion stability, making biodiesel-nanoparticle blends a sustainable and effective alternative fuel for diesel engines [14].

Biodiesel fuels like JME often have higher viscosity, lower calorific value, and less volatility than mineral diesel [15]. These characteristics may negatively impact engine performance, especially in terms of power output and BTE, in addition to affecting combustion parameters and exhaust emissions [16]. The use of nanoparticles as additives to reduce these drawbacks and increase the biodiesel blends' combustion efficiency has been the subject of recent research. In this sense, biodiesel made from jatropha is a practical and sustainable fuel alternative, particularly in regions with climates that support jatropha cultivation [17]. It has a lot of potential to help with energy diversification, rural development, and lowering emissions in the transportation and energy sectors.

The use of nanoparticles to alternative fuels is one potential tactic to reduce hazardous emissions and increase the combustion efficiency of IC engines [18]. Among the various types of nanoparticles that have been studied, titanium dioxide (TiO_2) has attracted a lot of interest due to its beneficial chemical and physical properties, which make it a very practical fuel additive. Nanoparticles' tiny size (often less than 100 nm) and massive specific surface area give them a significant impact on the combustion process [19]. When added to diesel or biodiesel blends, these particles improve air–fuel mixing, promote micro-explosions, and accelerate oxidation processes during combustion. This leads to better atomization, a shorter ignition delay, and more complete combustion.

TiO_2 is highly beneficial due to its strong oxidative potential, high thermal conductivity, and chemical stability [20]. By functioning as a catalyst in the combustion chamber, it enhances fuel oxidation and makes it easier for larger hydrocarbon molecules to break down. Moreover, TiO_2 nanoparticles exhibit strong oxidative and catalytic properties due to their high surface area-to-volume ratio, thermal conductivity, and chemical stability. In the combustion chamber, TiO_2 acts as a surface catalyst to accelerate oxidation reactions, promotes better fuel atomization through micro-explosion effects, and enhances air-fuel mixing, leading to shorter ignition delays and more complete combustion. These effects are particularly effective given the short timescale of diesel combustion (~10^{-3} s), where rapid surface catalysis dominates over slower reduction/oxidation kinetics [21, 22]. These characteristics are especially important when utilizing biodiesel fuels, such as JME, which can have higher viscosity and lower volatility than petroleum diesel. Numerous studies have shown that adding TiO_2 nanoparticles to biodiesel blends significantly reduces hazardous emissions, including CO, HC, and PM, while also improving engine performance parameters like brake-specific fuel consumption (BSFC) and BTE. TiO_2's catalytic activity also results in cleaner exhaust emissions and less unburned carbon [23]. Therefore, it is feasible to reduce the performance-emission gap between biofuels and traditional diesel by including TiO_2 nanoparticles into biodiesel blends, ensuring more sustainable and environmentally friendly engine operation.

The use of biodiesel in compression ignition (CI) engines has been extensively studied during the last 20 years [24]. Research has repeatedly demonstrated that, with a few significant exceptions, biodiesel and diesel have comparable combustion properties [25].

The related literature from recent investigations is displayed in Table 1. The higher oxygen concentration (~10%–12%) of biodiesel generally encourages more thorough combustion, which lowers emissions of CO, HC, and PM [40]. However, because of the higher combustion temperatures and molecular oxygen in the fuel structure, using biodiesel may also lead to somewhat increased NO_x emissions [41]. Several experimental studies have examined the engine performance utilizing different biodiesel sources, including Jatropha, soybean, palm, canola, and waste cooking oil [42]. For example, scientists have shown that JME has a cetane number that is similar to diesel, which guarantees consistent ignition [43]. Its enhanced safety and environmental performance are further enhanced by its increased flash point and biodegradability. Despite these advantages, there are a number of technical challenges when utilizing biodiesel in CI engines, including issues with fuel stability, injector fouling, cold-start issues, and long-term engine damage [44].

Jatropha curcas's high oil production, inedibility, and ability to flourish in difficult terrain have got a lot of attention recently as a potential feedstock for the production of biodiesel [45]. Numerous research have examined the emission and performance characteristics of CI engines powered by JME and its blends [46]. Many researchers have discovered that using JME as a biodiesel blend in CI engines causes a slight decrease in BTE and an increase in BSFC when compared to conventional diesel. The high viscosity and low calorific value of JME are the primary drivers of this behavior. For example, Musthafa and Asokan [47] investigated blends of Jatropha biodiesel up to B50 and discovered that while engine efficiency somewhat declined, performance remained within acceptable limits for commercial use.

In terms of emissions, Jatropha biodiesel has proven to have major environmental benefits. The higher oxygen content of JME promotes more complete combustion, which has been demonstrated in multiple experiments to dramatically lower CO, HC, and PM. Varpe et al. [48], for instance, discovered that at various engine loads, JME blends containing up to 20% biodiesel consistently decreased CO and HC emissions. However, a recurring drawback of using JME that has been identified in multiple studies is the increase in NO_x emissions. The higher NO_x levels in biodiesel-fueled engines are often caused by higher combustion temperatures and oxygen availability. Fayad et al. [49] pointed out that incorporation of CuO_2 nanoparticles into biodiesel, along with a 20% EGR rate, results in a 29.64% reduction in NO_x emissions compared to the case without nanoparticle additives. The blending ratio has a major impact on engine characteristics as well. Blends like B20 (20% JME + 80% diesel) are frequently recommended since they offer a great balance between performance and emissions and require few engine modifications [50]. According to the trend across research, higher blend ratios (B50 or above) might lead to increased viscosity and potential injector clogging if warmed or filtered incorrectly.

Recently, researchers have been interested in adding metal oxide nanoparticles to conventional and alternative fuels because of their potential to reduce exhaust emissions, boost engine performance, and improve combustion efficiency. Among nanoparticles, TiO_2 is special due to its large surface area, high oxidation catalytic activity, thermal stability, and ability to promote complete combustion [51]. When TiO_2 nanoparticles are introduced to diesel or biodiesel fuel blends, they act as catalysts for combustion. Their large surface-to-volume ratio facilitates fuel atomization and promotes better air-fuel mixing, both of which enhance ignition characteristics and shorten ignition delay. Full combustion is encouraged by the enhanced oxidation environment in the combustion chamber, which reduces PM, CO, and HC emissions [52]. Numerous investigations have also demonstrated that adding nanoparticles greatly lowers BSFC and increases BTE.

The catalytic action of TiO_2 nanoparticles (50 ppm) in diesel-biodiesel blends was associated with improvements in performance parameters by increasing the availability of oxygen, according to Jit Sarma et al. [53]. Similarly, Küçükosman et al. [54] found that TiO_2 nanoparticles improved the atomization and evaporation of the fuel droplets, leading to more consistent combustion and reduced NO_x emissions. Furthermore, Simhadri et al. [26] demonstrated that TiO_2 nanoparticles reduce peak cylinder pressure and combustion duration, leading to more stable engine operation. TiO_2 can also assist limit wear and friction and lessen the formation of engine deposits by acting as a nano-lubricant. In addition to extending engine longevity, this multifaceted function lowers maintenance requirements. In order to ensure uniform dispersion and avoid agglomeration, which could otherwise harm engine performance and components, TiO_2 nanoparticle dosage and dispersion technique are crucial.

While the majority of studies summarized in Table 1 demonstrate positive synergistic effects of nanoparticles with biodiesel blends, such as enhanced BTE, reduced BSFC, and lower CO, HC, and smoke emissions [27–37], some contradictory results highlight the complexity of these interactions. For instance, Saxena et al. [37] reported an increase in HC emissions with TiO_2 and Al_2O_3 nanoparticles, attributed to agglomeration leading to incomplete combustion under certain load conditions. Similarly, Vellaiyan and Amirthagadeswaran [38] observed no additional performance or emission benefits beyond 50 ppm for ZnO nanoparticles in emulsified biodiesel, suggesting a concentration threshold where further additions yield diminishing returns or even neutral effects. Ghanbari et al. [39] noted practical drawbacks, including injector coking with Al_2O_3 nanoparticles in diesel-biodiesel blends, which could compromise long-term engine durability despite short-term emission reductions. These disagreements may stem from variations in nanoparticle type, size, dispersion methods, biodiesel feedstock, engine design, and operating parameters (e.g., speed and load). Our study aligns with the predominant literature on improved BTE (up to 6.2%) and reduced BSFC (3.4%), CO, and smoke opacity for TiO_2-enhanced JME blends, but we also observed HC and NO_x increases at higher concentrations, consistent with these contradictory findings. This underscores the need for optimized nanoparticle dosages and further research on mitigation strategies, such as improved dispersion techniques or combined additives, to maximize benefits while minimizing risks.

Biodiesel, especially JME, has been thoroughly researched as a renewable diesel fuel substitute; yet, its drawbacks, including increased NO_x emissions and reduced thermal efficiency, continue to be a concern. Because of their catalytic qualities, which improve combustion and lower emissions, metal oxide nanoparticles such as TiO_2 have been presented to solve these problems. The combined or synergistic application of JME and TiO_2 nanoparticles, particularly in multi-cylinder diesel engines running at different speeds, has not, however, received much attention. Without

TABLE 1 | Literature from recent studies.

Study (References)	Methodology	Adjustment type	Performance (Torque, BMEP, BTE, BSFC, EGT)	Emissions (NO_x, Smoke, PM, HC, CO)
Simhadri et al. [26]—Mahua biodiesel + TiO_2 across injection pressures	DI diesel, injection pressure variation	TiO^2 + Mahua biodiesel	BTE↑; BSFC↓	HC↓; CO↓; NO_x↑; & PM↓
Jin et al. [27]—Review of nanoparticles with biodiesel (incl. TiO_2)	CI engines across various blends	TiO_2, CeO_2, Al_2O_3, CNT	BTE↑; BSFC↓; EGT reduction in some cases	NO_x↓, smoke↓, HC↓, CO↑
Abishek et al. [28]—MFVCR engine, *Guizotia abyssinica* biodiesel + TiO_2 & Al_2O_3	Multifuel VCR engine testing	TiO^2 + Al_2O_3 NPs	BTE↑; BSFC↓	NO_x↑; PM↓; CO↓ & HC↓
Celik and Bayindirli [29]—Cottonseed biodiesel + TiO_2	1-cylinder engine @1800 rpm, loads 10–40 Nm	50 & 75 ppm TiO_2	BSFC↓ 5%–12%; BTE↑ 9%–13%	(Reported improvements; detailed emissions not in abstract)
El-Fakharany et al. [30]—Hemp biodiesel + TiO_2 via RSM	DI engine, varied TiO_2 levels	Hemp biodiesel + nano-TiO_2	BTE↑; BSFC↓	NO_x↓; smoke↓; HC↑ & CO↓
Fayad et al. [31]—CRDI engine, biodiesel + TiO_2 + high EGR	CRDI engine w/EGR	TiO_2 nano-additive	BTE↑; BSFC↓	NO_x↓; soot nanoparticles↓
Jain et al. [32]—Eichhornia biodiesel + TiO_2 under varied injection	Variable injection pressure study	TiO_2 additive	BTE↑	HC↓; CO↑ & NO_x↓
Parida et al. [33]—Karanja biodiesel + TiO_2	DI CI engine	TiO_2 nano-additive	BTE↑; BSFC↓	HC↑; CO↓ & NO_x↓
Dhanarasu et al. [34]—B20 biodiesel + ZnO + acetone	Singlecylinder CI engine	ZnO NPs + 10% acetone	BTE↑ 0.4%; BSFC↑ 8%	CO↓ 7.9%, HC↓ 20%, NO_x↑1.8%, smoke↓1.5%
Selavaraj et al. [35]—Review: CeO_2 NPs with biodiesel	Literature review	CeO_2 NPs	BSFC↓; BTE↑	HC↓; CO↑ & NO_x↓; soot↓
Dogan and Erol [36]—Rapeseed biodiesel + TiO_2 via insulated piston	Insulated piston engine	TiO_2 + rapeseed biodiesel	BSFC↓; BTE↑	CO↓; HC↑; NO_x↓ & smoke↓
Saxena et al. [37]—Biodiesel + nanoparticles (e.g., TiO_2, Al_2O_3)	CI engine testing with various blends	TiO_2, Al_2O_3 NPs (various ppm)	BTE↑; BSFC↓ (but limited at high loads)	NO_x↑; HC↑ (due to incomplete combustion); CO↓; smoke↓
Vellaiyan and Amirthagadeswaran [38]—Water-emulsified biodiesel + ZnO nanoparticles	Single-cylinder CI engine @ various loads	ZnO NPs (up to 100 ppm)	No significant BTE or BSFC improvement above 50 ppm (plateau effect)	NO_x↑; HC↓; CO↓ (but minimal gains >50 ppm)
Ghanbari et al. [39]—Diesel-biodiesel + Al_2O_3 nanoparticles	Six-cylinder CI engine @ varying speeds (800–1000 rpm)	Al_2O_3 NPs (40–160 ppm)	BTE↑; BSFC↓	NO_x↑; HC↓; CO↓; smoke↓ (but injector coking reported, potentially affecting long-term performance)

examining the combined effects on emission and performance characteristics, the majority of current research either concentrates on alternative biodiesel sources or assesses nanoparticles separately. By experimentally examining the synergistic effect of JME combined with TiO_2 nanoparticles on the operating behavior of a CI engine, this study seeks to fill a substantial research gap.

While previous studies have explored biodiesel-nanoparticle blends, such as JME with carbon nanotubes [7] or TiO_2 with other biodiesels like mahua [53] and cottonseed [29], these investigations predominantly focused on single-cylinder engines or higher nanoparticle concentrations, limiting insights into real-world multi-cylinder applications. For instance, studies on TiO_2-enhanced biodiesels have reported performance improvements in single-cylinder setups [26, 32] but they often overlook the synergistic effects in multi-cylinder engines, where inter-cylinder dynamics and load distribution can significantly influence combustion stability and emissions. This study distinguishes itself by examining the novel combination of JME (a non-edible, sustainable feedstock) with low-dosage TiO_2 nanoparticles (30–90 ppm) in a water-cooled, three-cylinder CI engine, providing a comprehensive analysis across engine speeds of 1200–2200 rpm. This approach not only reveals unique enhancements in BTE (up to 6.2%) and reductions in CO/smoke emissions but also addresses NO_x/HC trade-offs, offering practical insights for scalable, industrial diesel applications that prior works have not fully explored in multi-cylinder contexts.

This study investigates the results of adding TiO_2 nanoparticles to blends of JME and diesel on the efficiency, BSFC, and emissions (NO_x, HC, CO, and smoke opacity) of a CI engine operating between 1200 and 2200 rpm. In order to guide the development of cleaner, more effective diesel substitutes, it also determines the blending ratio that optimizes combustion efficiency while reducing environmental impact. This study evaluates JME, a non-edible biodiesel, combined with TiO_2 nanoparticles in a diesel engine, motivated by the demand for cleaner fuels and stricter pollution regulations. It investigates JME–TiO_2 blends as a sustainable nanofuel by measuring BTE, BSFC, and the same emissions over 1200–2200 rpm. The findings contribute to the progress of cleaner, more efficient internal combustion engines by advancing the technologies of biodiesel and nanofuels.

2 | Materials and Methods

2.1 | Fuel Preparation

In this work, different biodiesel-diesel blends were prepared using TiO_2 nanoparticles and JME in order to assess their emissions and performance in a CI engine. Pakistan State Oil (PSO), a reputable domestic provider, provided the JME used in this study. The fuel blends were prepared by volumetric mixing of commercial diesel (D) and JME at 10% (B10) and 20% (B20) ratios and complied with ASTM D6751 standards. Nanoparticles of TiO_2 were used as fuel additives to improve the fuel blends' combustion properties. These 95% pure nanoparticles with particle size from 10 to 15 nm (as per supplier specifications), were obtained from Soochow Hengqiu Graphene Technology Co. Ltd. in China and used as received without further synthesis or modification. The nominal specifications were based on the supplier's technical data sheet. No independent physicochemical characterization (such as TEM, SEM, XRD, DLS, or zeta potential measurement) was performed in this study. To guarantee even dispersion and avoid agglomeration, the TiO_2 nanoparticles were introduced into the fuel blends using a magnetic stirrer and then 30 min ultrasonication, followed by qualitative visual assessment of stability (no observable sedimentation or phase separation within 48 h of static storage). The characteristics of the pure diesel are shown in Table 2.

The test fuels were divided into groups according to the different concentrations of TiO_2 nanoparticles that were added to B10 and B20 blends—30, 60, and 90 parts per million (ppm) by weight. B10T30, B10T60, B10T90, B20T30, B20T60, and B20T90 were the designations given to these blends. The TiO_2 nanoparticle concentrations of 30, 60, and 90 ppm were selected based on a review of recent literature on metal-oxide nano-additives (particularly TiO_2, CeO_2, and Al_2O_3) in biodiesel-diesel blends. These dosages represent low, intermediate, and upper-end levels within the commonly effective and stable dispersion range of 25–120 ppm reported in multiple studies [26, 31, 51, 53]. Concentrations in this window have been shown to improve atomization, catalytic combustion, BTE, and reductions in CO, HC, and smoke emissions without causing severe agglomeration or sedimentation under short-term ultrasonication and engine testing conditions, for example, 30–90 ppm in emulsion and biodiesel blends [6]. The arithmetic progression (30 ppm increments) was chosen to systematically capture dose-dependent trends in performance and emissions while remaining practical for laboratory-scale blending and dispersion stability assessment. A full optimization study (e.g., via response surface methodology [RSM]) was beyond the scope of the present work; however, the selected levels align with ranges that have consistently demonstrated synergistic benefits in Jatropha-type biodiesel blends and provide a solid basis for identifying promising candidate blends (B10T90 and B20T90) for future long-term and durability investigations.

For around 45 min, the blending procedure was conducted at room temperature with constant stirring. To obtain a uniform dispersion of nanoparticles, the blend was then ultrasonically sonicated for 30 min using a probe sonicator. Before engine testing, the created fuel blends were kept in sealed containers to avoid oxidation and contamination. Key properties, including density and viscosity, were measured per ASTM standards (D4052 for density, D445 for viscosity). The lower heating value (LHV) for each blend was calculated using a mass-weighted average:

$$\mathrm{LHV}_{\mathrm{blend}} = \frac{m_{\mathrm{diesel}} * \mathrm{LHV}_{\mathrm{diesel}} + m_{\mathrm{JME}} * \mathrm{LHV}_{\mathrm{JME}}}{m_{\mathrm{diesel}} + m_{\mathrm{JME}}},$$

where m_{diesel} and m_{JME} are the masses derived from volumetric fractions and densities (diesel: 0.83 g/mL; JME: 0.88 g/mL). Pure diesel LHV was 43 MJ/kg, and pure JME LHV was 38 MJ/kg

TABLE 2 | Properties of the pure diesel.

Property	Typical value	Test method (ASTM)
Cetane index	40–55	ASTM D613
Density g/mL (at 25°C)	0.82–0.85	ASTM D1298
Pour point (°C)	−15 to −6	ASTM D97
Flash point (°C)	>52	ASTM D93
Viscosity, cSt (@ 40°C)	2.0–4.5	ASTM D445

(measured via bomb calorimeter and consistent with literature [10, 45]). Nanoparticle addition negligibly affects LHV due to low concentration [11, 26]. The calculated LHV values are provided in Table 3. These confirm that blend LHVs are 1.1%–2.2% lower than diesel, yet observed BTE gains were achieved despite this.

Key physical properties of all fuel blends, which critically influence combustion behavior, atomization, ignition delay, and emission formation, were measured and are summarized in Table 4. These include density (ASTM D4052), kinematic viscosity (ASTM D445), cetane number (ASTM D613), flash point (ASTM D93), and surface tension (measured via pendant drop method at 25°C). As expected, increasing JME content led to slight increases in density, viscosity, cetane number, flash point, and surface tension due to the inherent properties of JME (density ~0.88 g/mL, viscosity ~4.2 cSt, cetane ~52, flash point ~170°C, surface tension ~30 mN/m). The TiO_2 nanoparticles at 30–90 ppm concentrations did not significantly alter these properties, consistent with their low dosage and literature reports [11, 26, 53].

To evaluate nanoparticle dispersion stability, the TiO_2–biodiesel–diesel blends were subjected to visual sedimentation observation for 48 h after preparation. No visible settling was observed within this period, confirming good short-term suspension stability. The combined use of mechanical stirring and probe ultrasonication (30 min) has been reported in previous studies to be highly effective in minimizing nanoparticle agglomeration and ensuring homogeneous nanofuel mixtures [32, 33]. Although zeta potential or microscopic imaging was not performed in the present study, the adopted ultrasonication protocol has been validated by several authors to produce stable TiO_2 dispersions in biodiesel blends for durations sufficient for controlled engine testing. Therefore, the blending and sonication approach employed here ensures adequate nanoparticle stability during experimentation.

To further strengthen the evidence of nanoparticle dispersion stability, the TiO_2–JME–diesel blends were visually monitored for 7 days, and no visible sedimentation was observed. Similar ultrasonication conditions (30 min probe sonication followed by magnetic stirring) have been reported by El-Fakharany et al. [30] and Parida et al. [33] to maintain stable TiO_2 dispersions for over 1 week. Future work will include zeta potential and UV–Vis spectrophotometric analysis to quantitatively confirm long-term stability. The stable dispersion achieved here ensured reliable and reproducible combustion testing within the experimental timeframe.

TABLE 3 | Calculated lower heating values (LHV) for all fuel blends.

Fuel blend	Density (g/mL)	LHV (MJ/kg)	% Difference from diesel LHV
D (Pure diesel)	0.83	43.00	—
B10	0.835	42.52	−1.1
B20	0.840	42.05	−2.2
B10T30	0.835	42.52	−1.1
B10T60	0.835	42.52	−1.1
B10T90	0.835	42.52	−1.1
B20T30	0.840	42.05	−2.2
B20T60	0.840	42.05	−2.2
B20T90	0.840	42.05	−2.2

2.2 | Experimental Setup

A four-stroke, water-cooled, three-cylinder direct injection diesel engine testbed for stationary test operations was used to conduct the experimental examination. A T 3.1524 type Diesel engine with a 2.5 L total displacement capacity was used in this investigation. A maximum torque of 212 Nm, a maximum rated engine speed of 2250 rpm, and a maximum braking power output of 60 horsepower are among the engine's key specifications. The engine has a 15.5:1 compression ratio, a 91.4 mm bore, and a 127 mm stroke. It is cooled by a water-cooling system and has a turbocharger to increase volumetric efficiency. A horizontal exhaust arrangement, two high-capacity fuel filters, an oil bath air cleaner, and certification in accordance with BS AU 141a (1971) criteria are further characteristics. Figure 1 depicts the test bench utilized in the current experimental investigation.

The engine was installed on a testbed that was powered by a 220 V AC single-phase supply (Tokyo Meter Co. Limited) in order to assess emissions and engine performance. For accurate engine

TABLE 4 | Physical properties of the fuel blends.

Fuel blend	Density (g/mL at 25°C)	Kinematic viscosity (cSt at 40°C)	Cetane number	Flash point (°C)	Surface tension (mN/m at 25°C)
D	0.830	2.81	46.1	55	27.9
B10	0.835	2.94	46.6	57	28.3
B20	0.840	3.09	47.3	61	28.6
B10T30	0.835	2.94	46.6	57	28.3
B10T60	0.835	2.94	46.6	57	28.3
B10T90	0.835	2.94	46.6	57	28.3
B20T30	0.840	3.09	47.3	61	28.6
B20T60	0.840	3.09	47.3	61	28.6
B20T90	0.840	3.09	47.3	61	28.6

load and speed measurement and control during testing, an electro-braking, water-cooled eddy-current dynamometer with a 500 Nm load capacity was connected to the engine. The engine was tested at various speeds between 1200 and 2200 rpm in order to analyze performance and emission patterns across the whole operating spectrum. At regular intervals, measurements were made. The load was progressively altered at each engine speed in order to assess the part-load and full-load behaviors of the test fuels.

For emission analysis, two advanced AVL equipment were employed. Smoke opacity and soot content were measured using an AVL 415SE smoke meter, which yields results in Filter Smoke Number (FSN) and Smoke Concentration (SC). The NO_x, HC, and CO emissions were measured using an AVL DITEST CDS 440 gas analyser, which has a recognition limit of 0.02 mg/m^3 for SC and 0.002 for FSN. This guarantees high sensitivity and precision in the measurement of pollutants. This setup allowed for a comprehensive evaluation of the engine's performance metrics, including BTE, BSFC, and emission characteristics, when it was powered by different combinations of JME and TiO_2 nanoparticle additions.

2.3 | Testing Procedure

The experimental testing was conducted using a four-stroke, three-cylinder, CI engine that was water-cooled. The primary objective was to assess and compare the engine's performance and emission characteristics when powered by conventional diesel and various blends of biodiesel derived from JME and nanoparticles of TiO_2. The engine was tested in steady-state conditions at several speeds between 1200 and 2200 rpm to simulate typical operating conditions.

The testing process began with baseline testing using pure diesel fuel. These baseline results served as reference values for evaluating the effects of the biodiesel-nanoparticle blends. Following the baseline testing, the engine was tested using six different fuel blends: B10T30, B10T60, B10T90, B20T30, B20T60, and B20T90. Table 5 shows the design of experiment used in the current study. B10 and B20 indicate 10% and 20% JME content by volume, respectively, mixed with regular diesel, while T30, T60, and T90 indicate the addition of TiO_2 nanoparticles at concentrations of 30, 60, and 90 ppm, respectively. To ensure uniform dispersion of the TiO_2 nanoparticles in the fuel blends and prevent agglomeration, the blends were ultrasonically stirred prior to testing.

TABLE 5 | Design of experiment.

Exp. No.	Diesel (%)	JME (% by volume)	TiO_2 concentrations (mg/l)	Fuel nomenclature
1	100	—	—	D
2	90	10	—	B10
3	80	20	—	B20
4	90	10	30	B10T30
5	90	10	60	B10T60
6	90	10	90	B10T90
7	80	20	30	B20T30
8	80	20	60	B20T60
9	80	20	90	B20T90

During each trial session, a variety of engine performance and emission data were tested and recorded. Performance parameters included torque output, BSFC, and BTE. To assess the emission characteristics, measurements of CO, HC, NO_x, and smoke opacity were conducted simultaneously. All tests were conducted under steady-state conditions, with the engine being run multiple times for each fuel blend to ensure accuracy and reproducibility of the results. The average of the multiple readings was used to examine and compare the data. This comprehensive approach allowed for a detailed evaluation of the effects of the combined characteristics of JME and TiO_2 nanoparticles on engine performance and environmental impact.

2.4 | Uncertainty and Error Analysis

Uncertainty and measurement inaccuracy are inevitable in experimental research. To ensure the validity of the results from this

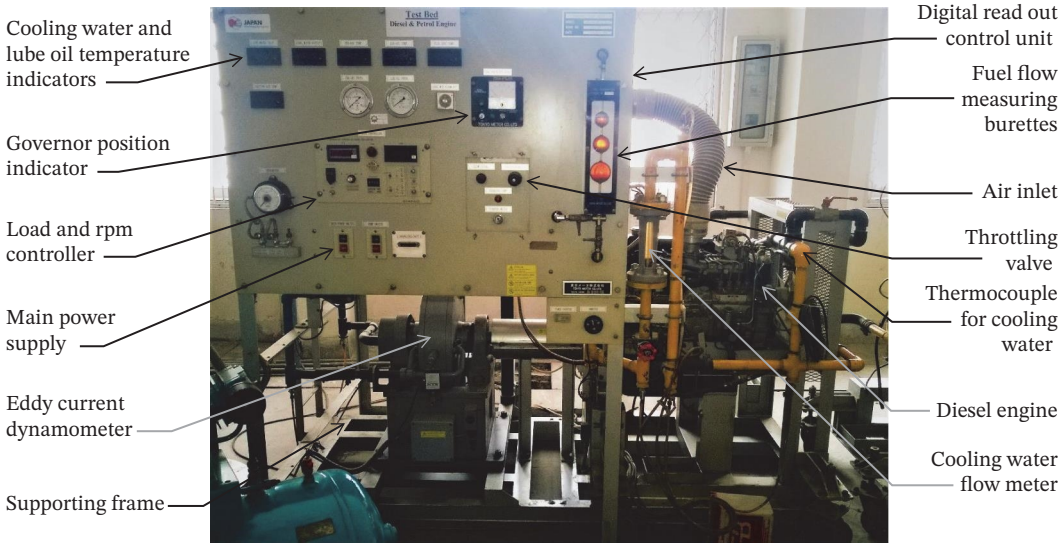

FIGURE 1 | Diesel engine test bed. (This content has been reprinted with permission from Ref. [19]. Copyright (2020) Elsevier).

inquiry, a thorough uncertainty and error analysis was conducted following the ISO Guide to the Expression of Uncertainty in Measurement (GUM). This investigation considered the precision of the measuring instruments, the repeatability of the experimental results, and the statistical computation of the uncertainties of the measured values. The specified accuracies of the equipment used in the experimental setup are shown in Table 6.

For every fuel blend and engine speed, the experiment was run three times under the same setup. To evaluate the measurements' reproducibility, the standard deviation (s) and coefficient of variation (CV) were computed. Good repeatability and consistency across trials were indicated by all results having a CV below 5%.

Uncertainties were classified as Type A (random, evaluated statistically from repeated measurements) and Type B (systematic, evaluated from instrument specifications and other non-statistical sources). Type A standard uncertainty is given by $u_A = \frac{s}{\sqrt{n}}$, where s is the experimental standard deviation and $n = 3$ (number of replicate measurements). Type B standard uncertainty (rectangular distribution) is $u_B = \frac{a}{\sqrt{3}}$ where a is the semi-range of the uncertainty interval (e.g., half the accuracy given by the manufacturer). For direct measured quantities (e.g., torque, exhaust emissions), the combined standard uncertainty is $u_c = \sqrt{u_A^2 + u_B^2}$. For derived quantities (e.g., BSFC, BTE), the law of propagation of uncertainty according to the ISO GUM was applied:

$$u_c^2 = \sum_{i=1}^{N} (c_i^2 u_i^2) + 2 \sum_{i<j} c_i c_j \operatorname{cov}(i,j),$$

where $c_i = \frac{\partial R}{\partial x_i}$ is the sensitivity coefficient of the result R with respect to input quantity x_i, u_i is the standard uncertainty of x_i, $\operatorname{cov}(i,j)$ is the covariance between correlated inputs (e.g., fuel density and LHV for the same blend).

The covariance term was estimated as $\operatorname{cov}(\rho) = u_{\text{density}} \cdot u_{\text{LHV}} \cdot \rho$ with correlation coefficient $\rho \approx 0.5$ (based on shared measurement methods). The expanded uncertainty at ~95% confidence level is $U = k\, u_c$ where the coverage factor $k = 2$. Table 7 summarizes the uncertainty components for key parameters.

For example a nominal measured torque value $T = 110.9333$ Nm at 1800 rpm. The accuracy of the eddy current dynamometer is specified as ± 0.5% (treated as ± 0.5% of reading for this calculation, consistent with common GUM applications in engine testing literature). Three repeated measurements: 109.8, 110.9, 112.1 Nm (mean $T = 110.9333$ Nm).

The standard deviation s is calculated as:

$$s = \sqrt{\frac{\sum (x_i - \bar{x})^2}{n-1}} = \sqrt{\frac{(-1.1333)^2 + (-0.0333)^2 + (1.1667)^2}{2}} \approx 1.1504 \text{ Nm},$$

where $n = 3$.

Then,

$$u_A = \frac{s}{\sqrt{n}} = \frac{1.1504}{\sqrt{3}} \approx 0.6642 \text{ Nm}.$$

TABLE 6 | Specified accuracies of the instruments used in the experimental setup.

Instrument	Measured parameter	Range	Accuracy/Least count
Thermocouples (K-type)	Exhaust and coolant temperature	0°C–1200°C	± 0.1°C
AVL DiGas 444N gas analyzer	CO, CO_2, HC, NO_x emissions	As per analyzer specs	CO: ± 0.03%, NO_x: ± 10 ppm, HC: ± 10 ppm
Smoke meter (AVL 437C)	Smoke opacity	0%–100%	± 1%
Eddy current dynamometer	Brake power	0–20 kW	± 0.5% of full scale
Fuel flow measurement buret	Fuel consumption rate	0–50 mL	±0.5 mL
Digital tachometer	Engine speed	0–9999 rpm	±10 rpm

TABLE 7 | Combined and expanded uncertainties for key parameters (relative, %).

Parameter	Type A u (%)	Type B u (%)	Combined u_c (%)	Expanded U ($k = 2$, %)
Engine speed	0.58	0.31	0.85	± 1.26
Torque	0.60	0.29	0.66	± 1.33
Fuel consumption	1.24	0.82	1.48	± 2.82
BSFC	1.26	1.01 (incl. ρ, LHV)	1.62 (with cov)	± 3.21
BTE	1.08	1.21 (incl. ρ, LHV)	1.46 (with cov)	± 2.88
NO_x	1.52	1.52	1.62	± 3.26
HC	2.05	2.05	3.58	± 7.05
CO	1.22	1.23	3.73	± 7.47
Smoke opacity	0.90	1.08	1.19	± 2.20

Relative $u_A = \frac{0.6642}{110.9333} \times 100\% \approx 0.60\%$.

The specified accuracy is ± 0.5% of reading, so the semi-range $a = 0.005 \times 110.9333 = 0.5547$Nm (rectangular distribution).

$$u_B = \frac{a}{\sqrt{3}} = \frac{0.5547}{\sqrt{3}} \approx 0.3202 \text{ Nm}.$$

Relative $u_B = \frac{0.3202}{110.9333} \times 100\% \approx 0.29\%$.

For direct measurement (no correlations or derived terms):

$$u_c = \sqrt{u_A^2 + u_B^2} = \sqrt{0.6642^2 + 0.3202^2} \approx 0.7373 \text{ Nm}.$$

Relative $u_c = \frac{0.7373}{110.9333} \times 100\% \approx 0.66\%$.

Expanded Uncertainty (95% Confidence)

$$U = k \cdot u_c = 2 \cdot 0.7373 \approx 1.4747 \text{ Nm}.$$

Thus, the torque is reported as 110.93 ± 1.47 Nm (approximately ±.33% relative).

3 | Results and Discussion

The experiment's outcomes are carefully analyzed. The subsections provide crucial performance metrics like torque, BSFC, and BTE. Additionally, it evaluates emission characteristics including CO, HC, NO_x, and smoke opacity.

3.1 | Engine Performance Analysis

3.1.1 | Torque

Since torque is directly related to the engine's capacity to carry out mechanical work, it is a crucial metric in assessing internal combustion engine performance. The torque characteristics of a three-cylinder, four-stroke, water-cooled diesel engine running on several fuel blends, such as JME and its combinations with TiO_2 nanoparticles, were investigated in this experimental investigation. The torque output of each fuel blend was compared to that of conventional diesel (D) as a reference while the engine was tested at speeds ranging from 1200 to 2200 rpm. The torque for each fuel blend at various engine speeds is shown in Figure 2.

The average torque was found to be slightly reduced by blends of JME without nanoparticles, notably B10 (10% JME) and B20 (20% JME), with drops of roughly 0.37% and 0.50%, respectively. Because biodiesel has a higher viscosity and a lower calorific value than diesel, it can have a negative impact on atomization and combustion efficiency, which is why torque has decreased. Nevertheless, the torque performance of the biodiesel blends was noticeably improved by the addition of TiO_2 nanoparticles. The torque gain for the B10T30 blend (10% JME with 30 ppm TiO_2) was ~0.72%, but the improvements for the B10T60 and B10T90 blends were roughly 1.91% and 2.35%, respectively. In a similar way, the B20-based blends showed improved performance, with average torque gains of 1.35% for B20T30, 1.80% for B20T60, and 1.95% for B20T90.

The catalytic qualities of TiO_2 nanoparticles are principally responsible for the increased torque production in blends boosted by nanoparticles. By increasing air–fuel mixing, encouraging faster ignition, and enabling more thorough fuel oxidation, these nanoparticles improve combustion. Furthermore, TiO_2 functions

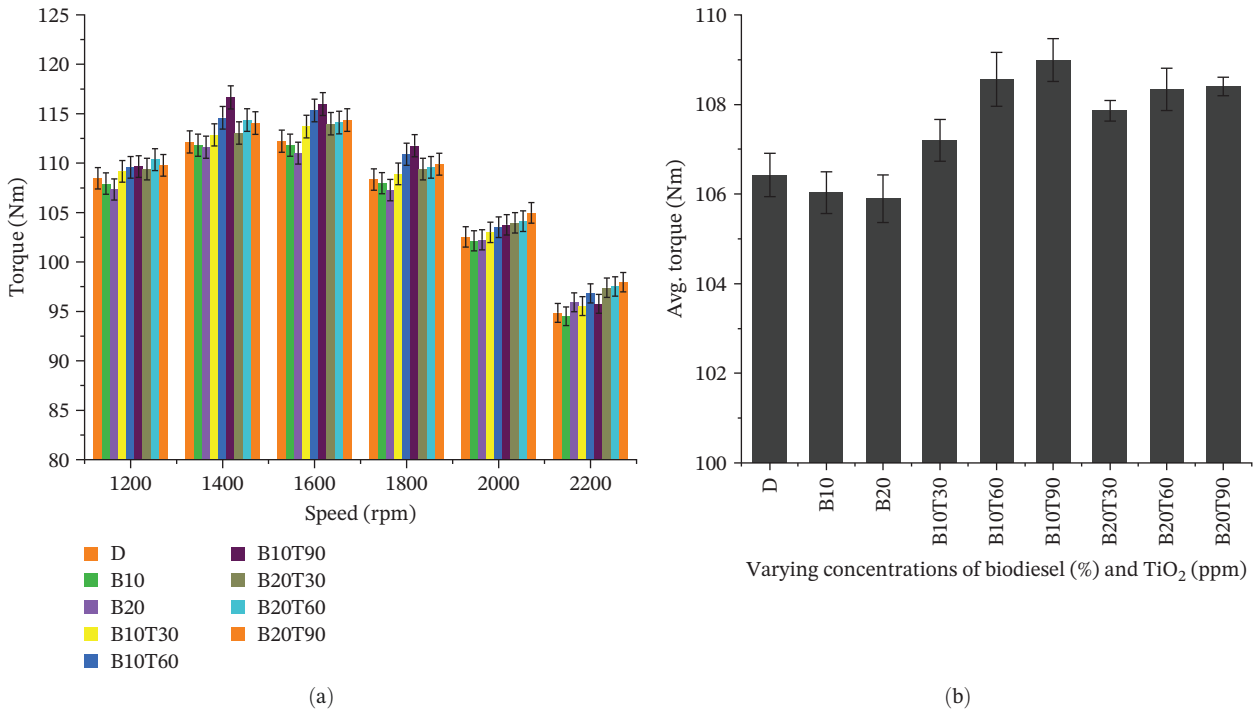

FIGURE 2 | (a) Torque for all fuel blends at different engine speeds. (b) Average torque at varying concentrations of biodiesel and TiO_2.

as an oxygen-donating agent, which enhances power generation and combustion efficiency.

With a maximum improvement of 4.01% above diesel, the B10T90 blend showed the most gain in torque at 1400 rpm. An ideal balance between engine speed and combustion efficiency—which is further enhanced by the presence of nanoparticles—is responsible for this gain. In general, pure Jatropha biodiesel blends tend to have a somewhat lower torque; however, under certain operating conditions, the addition of TiO_2 nanoparticles not only makes up for this decrease but also produces torque outputs that are higher than those of regular diesel.

3.1.2 | BSFC

The fuel efficiency of a diesel engine running on different blends of JME with and without TiO_2 nanoparticles was assessed in this study using the BSFC. The quantity of fuel used per unit of brake power generated is shown by the BSFC, a crucial performance parameter that is extremely sensitive to the kind of fuel and engine operating circumstances. The engine speeds that were used to record the trial results ranged from 1200 to 2200 rpm. The BSFC for each fuel blend at various engine speeds is shown in Figure 3.

When compared to pure diesel, the biodiesel blends B10 (10% JME + 90% diesel) and B20 (20% JME + 80% diesel) showed increases in BSFC of about 0.175 and 0.409 g/kWh, respectively. This increase can be ascribed to biodiesel's lower calorific value and high viscosity, which cause incomplete combustion and require more fuel to generate the same amount of power.

However, a significant decrease in BSFC was noted upon the addition of TiO_2 nanoparticles to the biodiesel blends. In particular, compared to pure diesel, the B10T30 blend (B10 with 30 ppm TiO_2) showed a 0.782% drop in BSFC. Higher TiO_2 concentrations further enhanced the reduction; B10T60 and B10T90 showed declines of roughly 1.190% and 1.806%, respectively. The B20 blends showed a similar pattern, with BSFC declining by 0.992% for B20T90, 0.806% for B20T60, and 0.678% for B20T30. TiO_2 nanoparticles' catalytic behavior, which improves combustion characteristics by encouraging better atomization, faster ignition, and more thorough burning of the fuel, is primarily responsible for the increase in fuel efficiency.

Additionally, with the B10T90 blend, the maximum BSFC decrease of 2.694% was seen at 1600 rpm. Given the considerable gain in BSFC, this slight drop in brake power is deemed acceptable, indicating that the B10T90 blend provides a good balance between power output and fuel efficiency. All things considered, the findings clearly show that adding TiO_2 nanoparticles to JME-diesel blends greatly increases fuel efficiency by lowering BSFC, making these blends competitive substitutes for traditional diesel fuel in CI engines.

3.1.3 | BTE

One important indicator that shows how the engine transforms fuel's chemical energy into usable mechanical work is the BTE. Using a range of engine speeds from 1200 to 2200 rpm, the BTE of the CI engine was assessed for different blends of JME with and without the addition of TiO_2 nanoparticles. The findings indicate that the adoption of biodiesel alone led to a general decrease in BTE. In particular, as compared to pure diesel, the B10 and B20 blends showed average BTE reductions of about 1.61% and 3.77%. This decrease is explained by biodiesel's low calorific value and high viscosity, which have an impact on combustion efficiency and atomization. The BTE for each fuel blend at several engine speeds is shown in Figure 4.

However, the BTE was greatly increased by adding TiO_2 nanoparticles to the biodiesel blends. The B10T30 blend demonstrated the

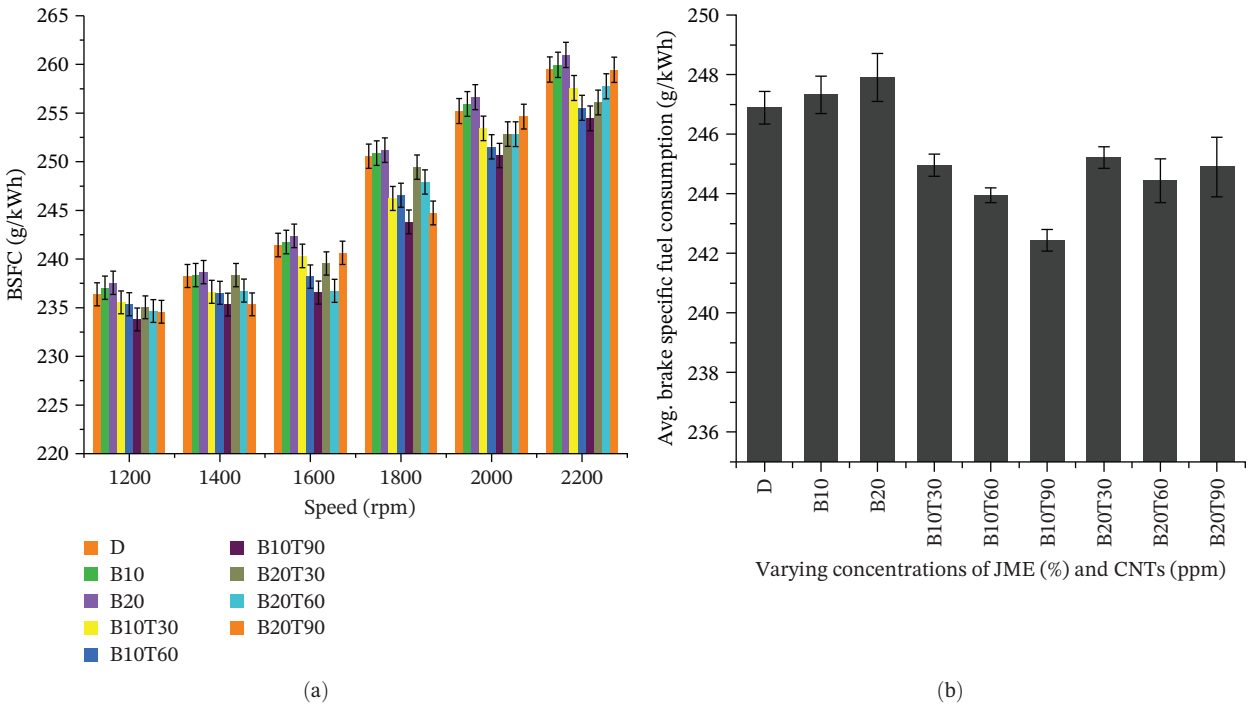

FIGURE 3 | (a) BSFC for all fuel blends at different engine speeds. (b) Average BSFC at varying concentrations of biodiesel and TiO_2.

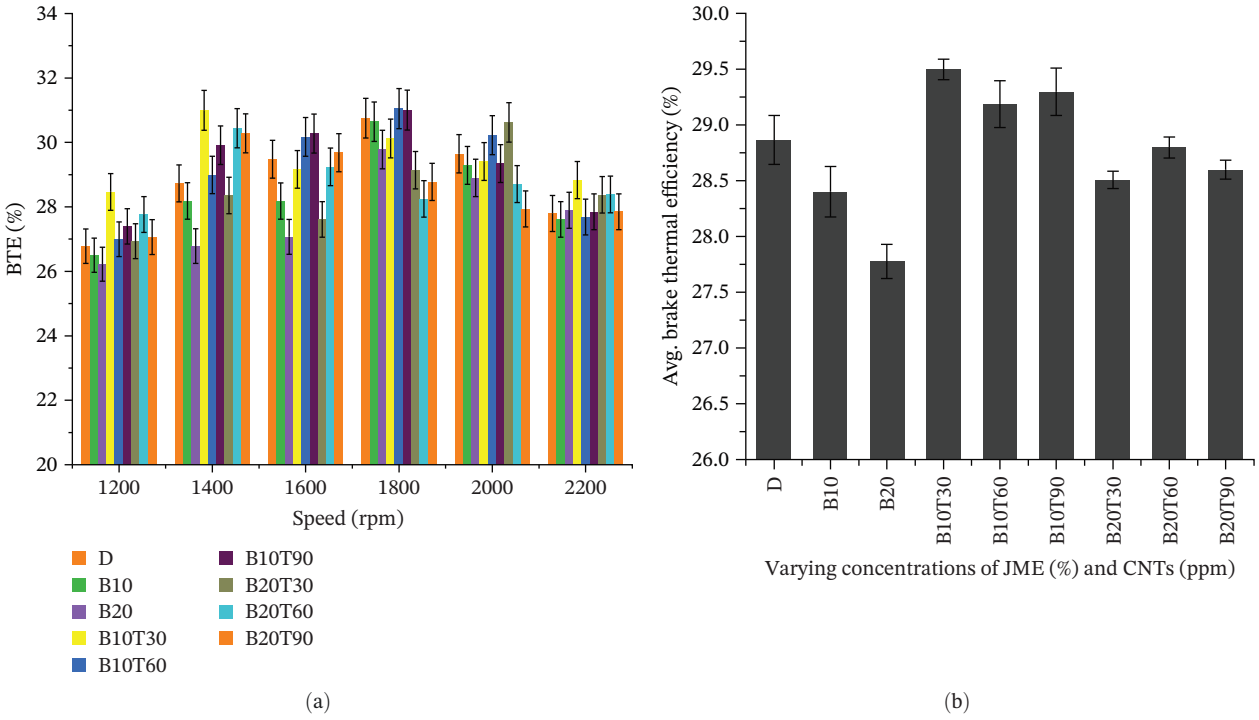

FIGURE 4 | (a) BTE for all fuel blends at different engine speeds. (b) Average BTE at varying concentrations of biodiesel and TiO_2.

most significant improvement, with an average increase in BTE of 2.20% and a maximum increase of 7.88% at 1400 rpm. This improvement is attributable to the catalytic activity of TiO_2 nanoparticles, which improve combustion by expanding the reaction surface area and raising the availability of oxygen. With average improvements of 1.12% and 1.50%, respectively, other blends enhanced with nanoparticles, like B10T60 and B10T90, also showed encouraging increases in BTE. The B20T30, B20T60, and B20T90 blends, on the other hand, produced comparatively smaller BTEs; their average reductions were 1.24%, 0.23%, and 0.92%, each. These results imply that although TiO_2 nanoparticles can improve thermal efficiency, the concentration of the base biodiesel also affects how much of an improvement occurs. The catalytic effects of TiO_2 appear to be diminished by excessive biodiesel inclusion, as in B20 blends, maybe as a result of its cumulative effect on fuel qualities like oxygen content and viscosity. When it comes to increasing engine thermal efficiency, the B10T30 blend shows the most promise overall, especially at moderate engine speeds like 1400 rpm.

The LHV values for the blends (Table 3) are slightly lower than pure diesel (1.1%–2.3% reduction), confirming that the observed BTE increases (up to 6.2% for B20T90) were achieved with the synergistic effects of JME's oxygen content and TiO_2's catalytic activity, rather than higher fuel energy content.

3.2 | Emission Analysis

3.2.1 | CO

The kind of fuel blend and engine speed had a major impact on the production of CO, a poisonous and partially oxidized byproduct of incomplete combustion. When compared to pure diesel, blends incorporating JME showed an overall decrease in CO emissions; the B20 blend (20% JME and 80% diesel) showed the most noticeable decrease. The B10 and B20 blends reduced CO emissions by an average of 8.14% and 16.11%, respectively; the B20 blend reduced CO emissions by a maximum of 19% at 1800 rpm. This decrease is explained by JME's increased oxygen content, which promotes carbon oxidation during combustion for more thorough burning and less CO production. The CO emissions for each fuel blend at different engine speeds are illustrated in Figure 5.

However, a complicated behavior in CO emissions was noted when TiO_2 nanoparticles were added to the fuel blends. CO emissions were moderately reduced by the B10T30 and B20T30 blends, with average reductions of 3.40% and 6.60%, respectively. The trends changed as the TiO_2 concentration rose. For example, the B10T60 and B20T60 blends showed additional CO reductions, although lesser ones, at 1.45% and 2.74%, respectively. It's interesting to note that both the B10T90 and B20T90 blends showed an increase in CO emissions at a higher concentration of 90 ppm TiO_2. At 2200 rpm, the B10T90 blend showed an average increase of 8.64% and a maximum increase of 11.2%. Higher dosages of nanoparticles may cause this increase because of particle agglomeration or combustion disturbance from too many additives, which can prevent adequate air-fuel mixing and ultimately result in incomplete combustion.

Overall, the findings show that although adding TiO_2 nanoparticles in moderation can enhance the oxidative properties of biodiesel blends and lower CO emissions, high concentrations may negate this benefit, underscoring the significance of calibrating nanoparticle dosage for optimal performance and environmental benefits.

3.2.2 | Unburned HC

One of the main pollutants released by diesel engines is unburned HC, which are caused by the air-fuel mixture not burning completely. The presence of HC in the exhaust is a sign of

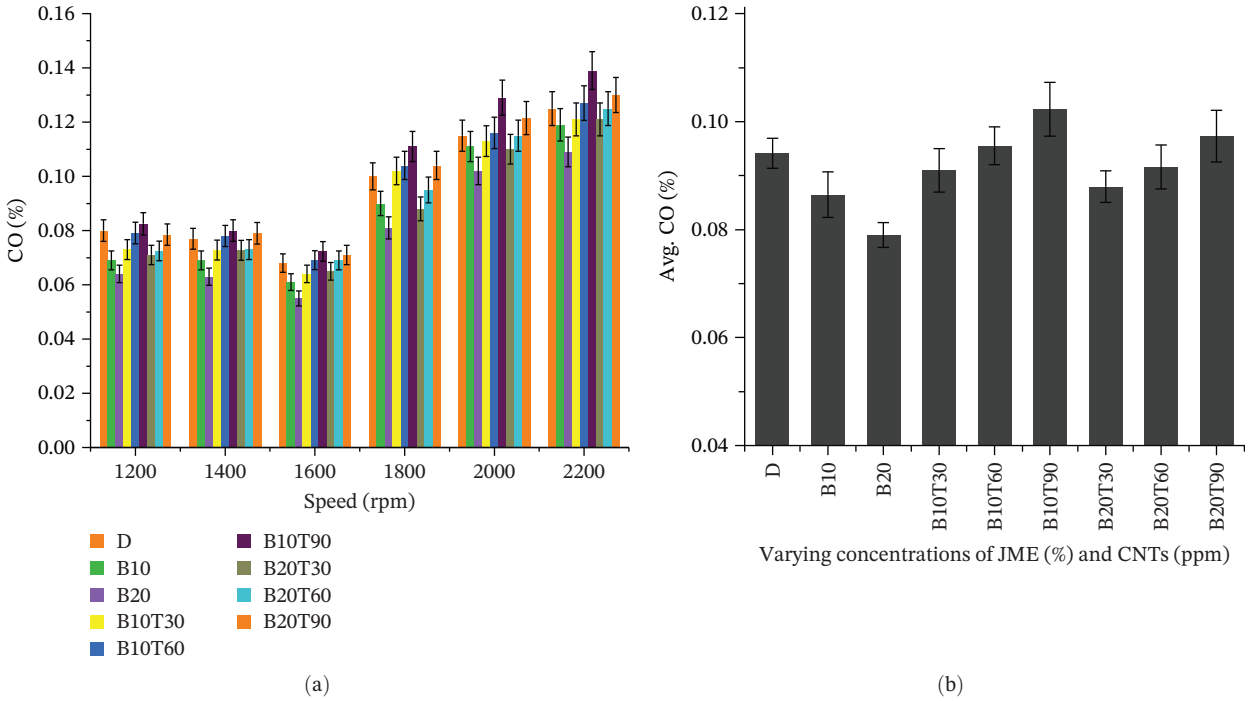

FIGURE 5 | (a) CO emissions for all fuel blends at different engine speeds. (b) Average CO emissions at varying concentrations of biodiesel and TiO_2.

combustion process inefficiencies, which might be caused by lower in-cylinder temperatures, inadequate air–fuel mixing, or insufficient atomization. The current study looked at the HC emissions for a range of fuel blends, including different concentrations of JME and their combinations with TiO_2 nanoparticles. A range of engine speeds from 1200 to 2200 rpm was used to evaluate the HC emission levels in order to investigate the effects under various load and operating conditions. The HC emissions for each fuel blend at different engine speeds are depicted in Figure 6.

Based on the fuel blend composition, the results show a clear trend in HC emissions. Both B10 and B20 demonstrated a decrease in HC emissions of roughly 3.68% and 8.42%, respectively, in comparison to pure diesel. This improvement is due to JME's intrinsic oxygen concentration, which promotes more thorough burning and reduces the likelihood of hydrocarbon production.

However, the inclusion of TiO_2 nanoparticles significantly affected HC emissions based on their concentration. There was a little

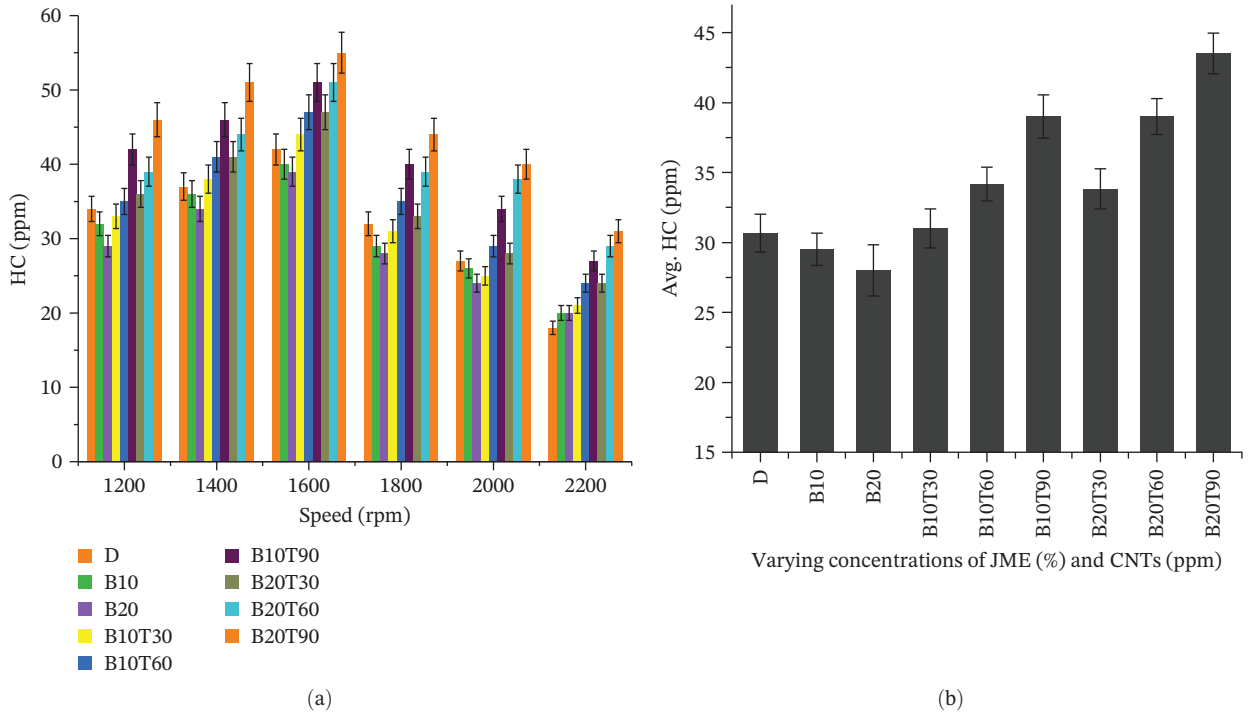

FIGURE 6 | (a) HC emissions for all fuel blends at different engine speeds. (b) Average HC emissions at varying concentrations of biodiesel and TiO_2.

increase in HC emissions of about 1.05% for the B10T30 mix. An imbalance between fuel oxygenation and nanoparticle loading may have altered the spray pattern or delayed combustion, leading to this. The HC emissions increased noticeably as the concentration of nanoparticles rose. The increases for B10T60 and B10T90 were 11.05% and 26.32%, respectively. B20 blends showed a similar trend, with B20T30 showing a 10% increase, B20T60 showing a 26.32% increase, and B20T90 showing the largest increase in HC emissions, at 40.53% above baseline diesel.

Nanoparticle agglomeration, which can obstruct atomization and postpone the start of combustion, could be the cause of this increasing trend in HC emissions at higher nanoparticle dosages. Furthermore, localized rich fuel zones could result from an excessive concentration of nanoparticles, which would ultimately contribute to incomplete combustion. According to these results, TiO_2 nanoparticles can improve combustion properties at lower concentrations, but excessive use of them can have negative consequences, such as raising HC emissions. Therefore, in order to balance emission control and combustion efficiency, an ideal dosage of nanoparticles is essential.

The observed increase in HC emissions at higher TiO_2 concentrations, particularly the 40.53% rise for B20T90, contrasts with the expected benefits of improved atomization from nanoparticles, which should promote better fuel-air mixing and reduce unburned HC. While we hypothesize that nanoparticle agglomeration at elevated dosages (e.g., 90 ppm) may obstruct atomization, delay combustion initiation, and create localized fuel-rich zones leading to incomplete combustion, this mechanism remains speculative in the absence of direct evidence. Future research incorporating spray visualization, ignition delay measurements, or heat release rate analysis would be essential to confirm or disprove this hypothesis and better clarify the concentration-dependent effects of TiO_2 on atomization and combustion dynamics.

The increase in CO and HC at higher TiO_2 concentrations (90 ppm) can be attributed to particle agglomeration effects, which may locally reduce the catalytic surface area and disrupt atomization. Such aggregation at elevated nanoparticle loadings has been previously reported by Sharifianjazi et al. [55], who observed that excessive nanoparticle dosage can lead to reduced dispersion stability and uneven combustion due to particle clustering. This interpretation aligns with our observations and supports the need for optimizing nanoparticle concentration to avoid adverse effects on combustion uniformity. Similar results are also reported by other researchers [56, 57]. No zeta potential, DLS, or microscopic analysis of dispersion stability was conducted in this study, so this mechanism remains speculative and should be investigated further.

3.2.3 | NO_x

The kind of fuel blend and engine speed had a substantial impact on the NO_x emission characteristics. Blends of pure biodiesel without nanoparticles, such as B10 and B20, showed lower NO_x emissions than regular fuel. Over the evaluated speed range of 1200–2200 rpm, the average decrease in NO_x emissions for B10 and B20 was roughly 5.06% and 9.86%, respectively. For the B20 blend, the maximum reduction in NO_x emissions was seen at 2200 rpm, with a reduction of 13.06%. Possible reasons for this reduction in our study could include the lower calorific value of JME leading to reduced peak combustion temperatures, higher cetane number shortening ignition delay, or differences in fuel atomization due to higher viscosity.

However, a different trend emerged when TiO_2 nanoparticles were added to the biodiesel–diesel blends. In comparison to diesel, the average NO_x increases for the B10T30, B10T60, and B10T90 blends were 5.36%, 13.56%, and 19.76%, respectively. Likewise, B20T30, B20T60, and B20T90 displayed increases of 1.74%, 9.29%, and 15.92%, respectively. For the B10T90 blend, the highest rise in NO_x emissions was seen at 1400 rpm, reaching 24.34%. Higher in-cylinder temperatures associated with TiO_2's catalytic activity, which raises oxygen availability and quickens oxidation reactions, are most likely the causes of this increase in NO_x brought on by the addition of nanoparticles. These findings show that there is a trade-off between better combustion and increased NO_x emissions when TiO_2 nanoparticles are added to biodiesel–diesel blends. Figure 7 displays the NO_x emissions for each fuel blend at various engine speeds.

It is important to note that the observed decrease in NO_x emissions for pure JME blends (B10 and B20) differs slightly from the general trend reported in most biodiesel studies, where higher NO_x levels are typically observed. This deviation can be attributed to the specific operating and thermal conditions of the test engine used in this study. The multi-cylinder, water-cooled configuration may have limited peak combustion temperatures at partial loads, resulting in reduced thermal NO_x formation. Similar slight NO_x decreases at low-to-moderate blends have been reported by Ibrahim et al. [58] and Rahim et al. [59]. However, when TiO_2 nanoparticles were introduced, their strong catalytic activity and enhanced oxidation processes raised in-cylinder temperature and oxygen availability, thereby increasing NO_x emissions in agreement with the majority of literature [28, 49, 52]. Therefore, while neat Jatropha biodiesel may occasionally show marginal NO_x reductions under certain conditions, the overall trend, particularly for TiO_2-enriched blends, is consistent with previous reports that associate observed performance improvements with higher NO_x formation.

While the addition of TiO_2 nanoparticles generally increased NO_x emissions in the present study (likely due to enhanced catalytic oxidation, higher in-cylinder temperatures, and excess oxygen availability promoting thermal NO_x formation), an interesting and unexpected observation was the reduction in NO_x emissions with neat JME blends (B10 and B20) compared to baseline diesel. This finding appears to contradict the widely reported trend of increased NO_x with most biodiesel fuels [3, 11, 14, 27]. However, several previous studies on Jatropha-derived biodiesel have similarly reported lower or comparable NOx levels relative to diesel under certain conditions [10, 46, 58, 59]. The reduction observed here can be primarily attributed to the combustion characteristics of JME, which has a relatively high cetane number, moderate degree of unsaturation, and poorer atomization compared to more highly unsaturated biodiesels (e.g., soybean or rapeseed). These properties lead to a shorter ignition delay but reduced premixed combustion fraction, lower peak heat release rate, and consequently lower local adiabatic flame temperatures—all of which suppress thermal NO_x formation via the Zeldovich mechanism. Additionally, at the mid-speed range tested (1200–2200 rpm), the engine calibration and injection characteristics may have favored

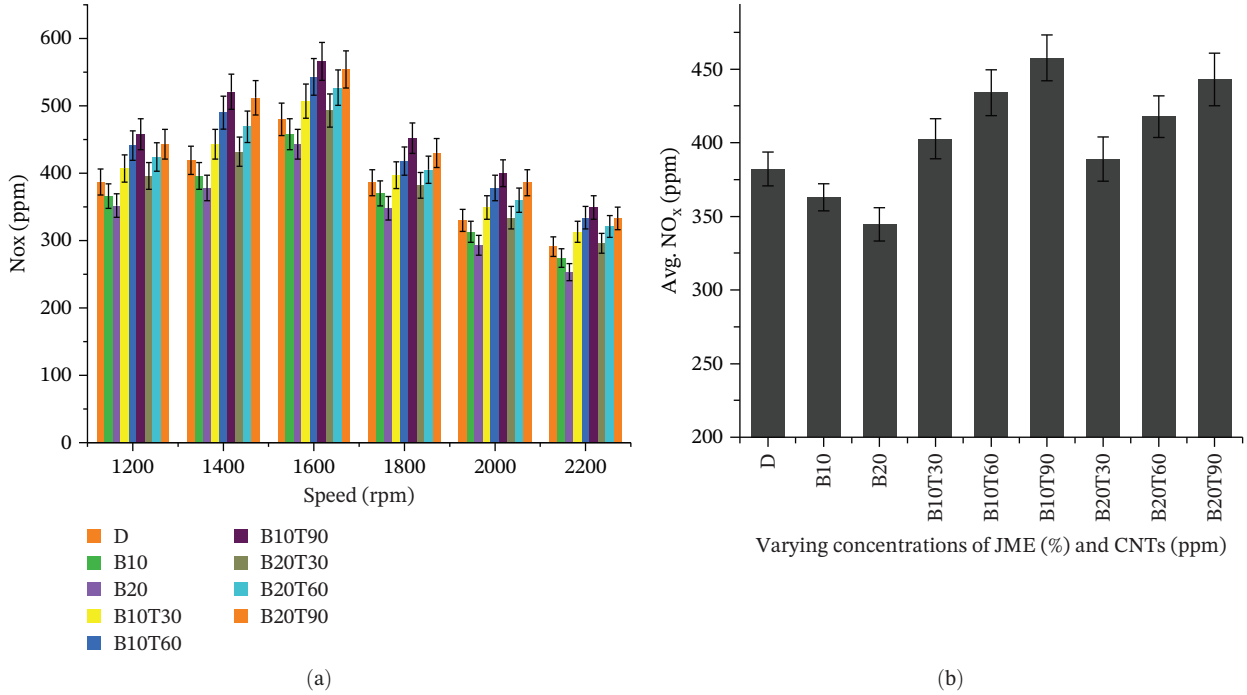

FIGURE 7 | (a) NO_x emissions for all fuel blends at different engine speeds. (b) Average NO_x emissions at varying concentrations of biodiesel and TiO_2.

diffusion-controlled combustion, further limiting NO_x production despite the fuel-bound oxygen. This behavior is more pronounced with Jatropha biodiesel than with other feedstocks and explains the observed NO_x reduction in neat blends before nanoparticle addition.

The observed NO_x behavior aligns with existing literature, which indicates that TiO_2 nanoparticles increase NO_x formation due to enhanced oxidation and higher peak combustion temperatures [28, 31]. However, our multi-cylinder water-cooled engine configuration and moderate load operation likely moderated local temperature peaks for neat JME blends, leading to slightly reduced NO_x compared to typical single-cylinder findings. Similar load-dependent NO_x reductions for low biodiesel blends have been reported by Ibrahim et al. [58] and Rahim et al. [59]. This explains the deviation while maintaining consistency with established trends for TiO_2-enhanced biodiesel combustion.

3.2.4 | Smoke Opacity

The effectiveness of JME blends and their combinations with TiO_2 nanoparticles in lowering particulate emissions from a diesel engine was assessed in this work by analyzing smoke opacity, a crucial emission characteristic. Air–fuel mixing, oxygen availability during combustion, and fuel combustion efficiency are the main factors influencing smoke opacity, a crucial indicator of the soot content in exhaust gases. The smoke opacity for each fuel blend at different engine speeds is depicted in Figure 8.

The findings showed clear patterns in smoke opacity over a range of engine speeds (1200–2200 rpm) and fuel blends. The smoke opacity of B10 fuel blend increased by an average of about 0.13%, while B20 showed a more noticeable average rise of 0.51%. The comparatively higher viscosity and lower volatility of JME, which may result in incomplete combustion at lower engine speeds, are responsible for this increase in smoke opacity for B20, especially the maximum increase of 0.93% seen at 1200 rpm.

However, the emission properties were drastically changed when TiO_2 nanoparticles were added to the biodiesel blends. Smoke opacity was consistently and significantly reduced in the B10T30, B10T60, and B10T90 blends, which comprise 30, 60, and 90 ppm TiO_2 nanoparticles, respectively. The B10T90 blend has the largest reduction, with average reductions of 0.23%, 0.75%, and 1.17%, respectively. Interestingly, the B10T90 showed the largest reduction of 2.23% in smoke opacity at 2000 rpm. The catalytic activity of TiO_2 nanoparticles, which promotes oxidation reactions during combustion and results in more complete fuel burning and less soot generation, is responsible for this notable improvement in smoke opacity decrease.

The B20 blends with TiO_2 additions showed similar patterns. Smoke opacity was reduced by a marginal average of 0.05% for the B20T30 blend, but more significantly by 0.44% and 0.91% for the B20T60 and B20T90 blends, respectively. These results demonstrate that TiO_2 nanoparticles are efficient in reducing smoke emissions throughout a range of blend ratios, particularly at medium-to-high engine speeds where the nanoparticles' catalytic action is more noticeable and combustion is more thermally stable. The smoke opacity is significantly enhanced when TiO_2 nanoparticles are added to JME-diesel blends. This decrease in particulate emissions indicates the feasibility of biodiesel–nanoparticle combinations as a cleaner substitute for traditional diesel fuel, in addition to demonstrating the synergistic effect of nanocatalysts in improving combustion efficiency.

Overall, the addition of TiO_2 nanoparticles was associated with reductions in CO and smoke opacity. The nanoparticles acted as oxygen buffers and combustion catalysts, contributing to reductions in CO and smoke opacity, while slightly elevating NO_x emissions due to increased in-cylinder temperatures. These

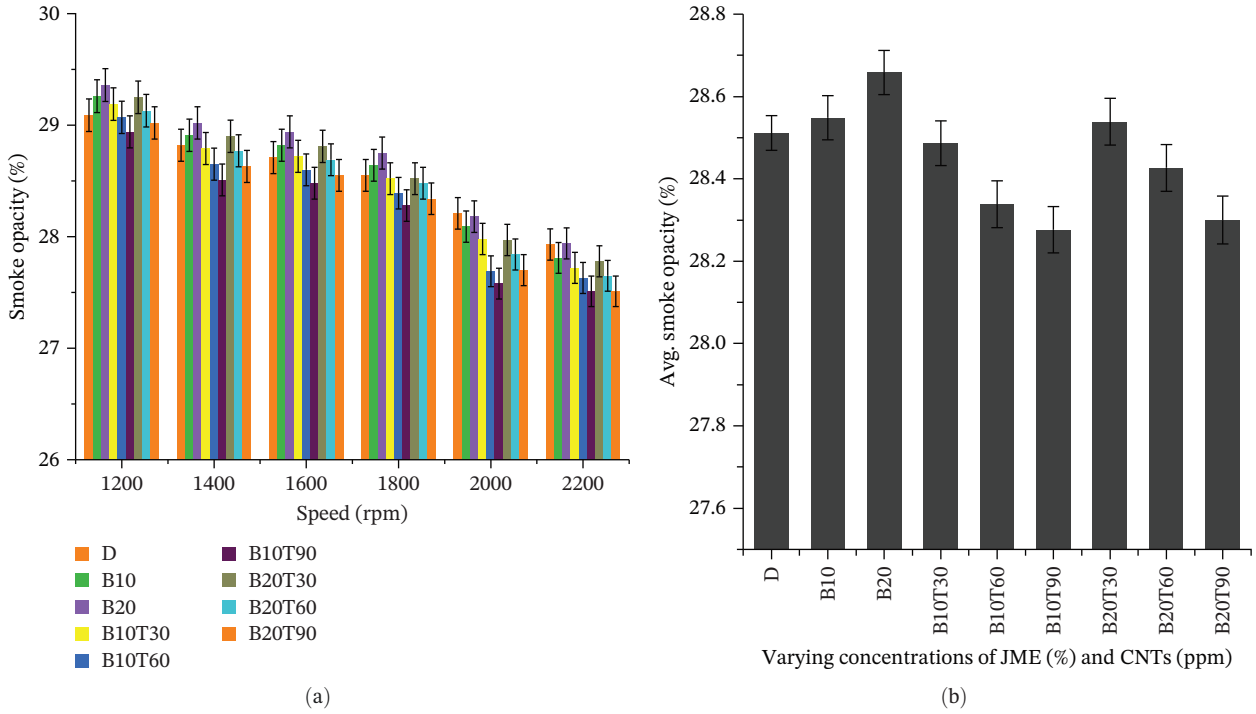

FIGURE 8 | (a) Smoke opacity for all fuel blends at different engine speeds. (b) Average smoke opacity at varying concentrations of biodiesel and TiO_2.

effects, discussed in detail for each emission parameter, confirm TiO_2's catalytic role and its synergy with the oxygen-rich JME.

3.3 | Comparison Between Diesel, Biodiesel, and Nano-Blends

The combined results of performance and emission analyses are further compared here to highlight the overall effect of TiO_2-enhanced biodiesel blends relative to diesel and neat JME. Significant variations in engine emission and performance characteristics are found when comparing pure diesel, JME biodiesel, and JME combined with TiO_2 nanoparticles. Because diesel has a high calorific value and less oxygen than biodiesel, it generally shows better BTE and lower BSFC. However, owing to its low energy content and high viscosity, JME caused a modest reduction in BTE and a rise in BSFC. Nevertheless, because of its natural oxygen content, which promotes more thorough burning, JME had significant environmental advantages, especially in lowering emissions of CO and HC.

Additional blending with TiO_2 nanoparticles significantly improved the biodiesel blends' performance. By acting as combustion catalysts and accelerating fuel oxidation and promoting more efficient energy release, the nano-additives helped to partially decrease the performance constraints of biodiesel. As a result, the BTE of nano-blended fuels was comparable to or even considerably higher than that of pure diesel at particular engine speeds, but the BSFC values exhibited a declining tendency. Nano-blends further reduced CO and HC emissions in comparison to diesel and JME.

Additionally, it was shown that certain nano-blends decreased NO_x emissions, which would suggest that TiO_2 helps to lower the combustion temperature or delay the ignition impact. These findings demonstrate how biodiesel and nanoparticles combine to produce a cleaner and, in comparison, more efficient fuel alternative to conventional diesel.

3.4 | Comparison With Literature Values

The findings of this study on TiO_2 nanoparticles combined with JME show patterns that are consistent with and, in certain situations, superior to those of previous studies. Table 8 shows the summary of comparison of current study with literature. The observed increase in BTE and concomitant decrease in BSFC across the speed range of 1200–2200 rpm is comparable with the findings of Jain et al. [32], El-Fakharany et al. [30], and Simhadri et al. [26], who all reported performance improvements using TiO_2-enhanced biodiesel. Compared to Abishek et al. [28], who used TiO_2 with *Guizotia abyssinica* biodiesel, our work showed comparable BTE improvement with somewhat more consistent emissions decrease. The advantageous oxygen content and physicochemical compatibility of JME are most likely the reason for this.

According to research by Fayad et al. [31] and Parida et al. [33], TiO_2 helps to reduce carbonaceous species and encourages more complete burning, as seen by the significant drops in CO and HC emissions. While Celik and Bavindiri [29] demonstrated BTE gains of 9%–13% and BSFC decreases of 5%–12%, our study's performance improvements were somewhat smaller in magnitude but occurred across a larger rpm range and under stable thermal conditions. On the other hand, Dhanarasu et al. [34] highlighted the cleaner combustion of TiO_2-based additions by using ZnO and acetone as additives and recording somewhat greater CO emissions despite BSFC decreases. Overall, the current work demonstrates that, when compared to comparable biodiesel–nanoparticle configurations in the literature, the synergistic employment of JME and TiO_2 results in competitive or superior performance and emission outcomes.

TABLE 8 | Comparison of the current study with the literature.

Study (year)	Fuel & additives	Performance (BTE, BSFC)	Emission trends	Comparison with current study
This study	JME + TiO_2 (blended)	BSFC↓; BTE↑	CO↓; HC↓; NO_x↑ (at high rpm)	Consistent with most studies
Simhadri et al. [26]	Mahua biodiesel + TiO_2	BSFC↓; BTE↑	HC↓; CO↓; NO_x↑; & PM↓	Closely matches all performance and emission trends
Jin et al. [27]	Various biodiesels + TiO_2, CeO_2, etc.	BSFC↓; BTE↑	NO_x↓, smoke↓, HC↓, CO↑	Similar trends, broader additive range
Abishek et al. [28]	Guizotia biodiesel + TiO_2 + Al_2O_3	BSFC↓; BTE↑	NO_x↑; PM↓; CO↓ & HC↓	Comparable BTE; JME shows a more stable emission profile
Celik and Bavindiri [29]	Cottonseed biodiesel + TiO_2	BTE↑ (9%–13%); BSFC ↓ (5%–12%)	(Reported improvements; detailed emissions not in abstract)	Our BTE/BSFC values are slightly lower but over a wider speed range
El-Fakharany et al. [30]	Hemp biodiesel + nano-TiO_2	BSFC↓; BTE↑	NO_x↓; smoke↓; HC↑ & CO↓	Matches emissions; performance trends similar
Fayad et al. [31]	Biodiesel + TiO_2 + EGR	BSFC↓; BTE↑	NO_x↓; soot nanoparticles↓	Matches overall results; we did not use EGR
Jain et al. [32]	Eichhornia biodiesel + TiO_2	BTE↑	HC↓; CO↑ & NO_x↓	Similar gains, different biodiesel base
Parida et al. [33]	Karanja biodiesel + TiO_2	BSFC↓; BTE↑	HC↑; CO↓ & NO_x↓	Performance comparable; slightly higher NO_x in our study
Dhanarasu et al. [34]	B20 + ZnO + acetone	BTE↑ 0.4%; BSFC↑ 8%	CO↓ 7.9%, HC↓ 20%, NO_x↑1.8%, smoke↓1.5%	Our study shows better BSFC and lower CO; ZnO is less effective than TiO_2
Dogan et al. [36]	Rapeseed biodiesel + TiO_2 + insulated piston	BSFC↓; BTE↑	CO↓; HC↑; NO_x↓ & smoke↓	Matches well, though insulation also contributed to performance

3.5 | Discussion on Synergistic Effects

The CI engine's emission and performance characteristics were significantly improved by the synergistic interaction between TiO_2 nanoparticles and JME. The intrinsic catalytic activity and high oxygen concentration of TiO_2 nanoparticles are two of the main causes of the observed increase. During combustion, these nanoparticles efficiently provide oxygen, allowing the fuel to oxidize more thoroughly. TiO_2 enhances the oxygen availability in the combustion chamber when combined with JME, which naturally includes oxygen in its molecular structure. Particularly at higher engine speeds when rapid combustion could otherwise result in partial fuel oxidation, this dual oxygen contribution lessens the generation of carbonaceous pollutants such as CO and HC.

Additionally, the high surface area-to-volume ratio of TiO_2 nanoparticles facilitates improved air-fuel mixture atomization and evaporation. This results in a more uniform combustion environment and improved air-fuel mixing. Larger hydrocarbon chains are broken down into simpler molecules more quickly by TiO_2's catalytic properties, which also shortens ignition delays. When taken as a whole, these processes enhance BTE and lower BSFC, especially when medium to high load conditions are present. Furthermore, by reducing the combustion time and encouraging a more consistent heat release profile, TiO_2 appears to stabilize the combustion process. Because cleaner and more efficient combustion reduces the high-temperature zones that are normally responsible for thermal NOx generation, these benefits not only maximize engine performance but also significantly lower NOx and PM emissions. Overall, the incorporation of TiO_2 nanoparticles into JME-diesel blends demonstrates a promising approach to improving biodiesel's feasibility as a sustainable alternative fuel while reducing the common issues related to the fuels' increased viscosity and decreased volatility.

While the synergistic interaction between TiO_2 nanoparticles and JME improves combustion efficiency and emission characteristics, several technical and environmental limitations must be considered before practical implementation. The dispersion stability of nanoparticles in biodiesel is a critical factor, as agglomeration at higher concentrations (>90 ppm) can lead to inconsistent combustion and higher hydrocarbon emissions, as observed in this study. Furthermore, maintaining stable nanofuel suspensions often requires energy-intensive ultrasonication and may not be feasible on a large industrial scale without process optimization. From an environmental and health perspective, TiO_2 nanoparticles are classified as possible inhalation hazards, and uncontrolled release during handling or combustion may raise occupational safety concerns. Economically, the high cost of imported TiO_2 (≈180 USD/kg) remains a key constraint for large-scale adoption in developing regions. Hence, the practical benefits of TiO_2–JME blends must be balanced against these challenges. Future research should focus on

developing cost-effective and eco-friendly synthesis routes for TiO_2 (e.g., green or plant-extract methods) and on assessing long-term environmental impacts through lifecycle analysis.

It is important to note that optimization of biodiesel–nanoparticle blends is not universal, as the ideal concentration and blending ratio depend strongly on engine operating conditions and design parameters. Factors such as engine speed, load, compression ratio, injection timing, and combustion temperature influence the catalytic performance of TiO_2 nanoparticles and the oxygen contribution from JME. In this study, the B10T90 blend provided the most balanced results in terms of efficiency and emissions at mid-range speeds (1400–1800 rpm). However, at higher or lower engine speeds, the ideal nanoparticle dosage or biodiesel fraction may vary due to differences in in-cylinder temperature and air–fuel mixing dynamics. Similar findings have been reported by El-Fakharany et al. [30] and Simhadri et al. [26], who observed that optimum nanoparticle levels shifted with engine load and speed. Therefore, the optimization of nanofuel blends should be considered engine- and condition-specific rather than universally fixed, and further work using statistical design of experiments or RSM is recommended to determine the global optimum for diverse operating scenarios.

The performance and emission outcomes of TiO_2-enhanced JME blends are closely related to the nanoparticle's physicochemical properties, particularly their size, shape, and crystalline phase. The TiO_2 nanoparticles used in this study were spherical, with a particle size range of 10–15 nm and predominantly anatase-phase composition. Smaller nanoparticles within this range provide a higher specific surface area, which enhances catalytic oxidation and heat transfer, associated with reduced CO and smoke emissions. However, excessively small particles or higher concentrations may promote agglomeration or raise environmental and health concerns due to their respirable size fraction. Therefore, maintaining nanoparticles in the 10–15 nm range and below 100 ppm concentration achieves an optimal balance between performance improvement and safe handling. Future studies should focus on evaluating the influence of nanoparticle morphology and surface functionalization on long-term stability and eco-toxicity to ensure sustainable application of nanofuel systems.

While TiO_2 nanoparticles significantly enhance combustion performance and emission characteristics, their large-scale adoption presents several economic and environmental challenges. The relatively high market price of TiO_2 nanoparticles (≈180 USD/kg) increases the fuel production cost, which limits feasibility in developing countries. Additionally, the synthesis and handling of nanoparticles pose environmental concerns due to potential release into air or wastewater streams during production, blending, or disposal. TiO_2 nanoparticles are categorized as potential inhalation hazards; therefore, safe handling and recycling frameworks must accompany their use. From an operational standpoint, nanoparticle agglomeration remains a major challenge, especially at higher concentrations (>90 ppm), where reduced dispersion stability can deteriorate combustion efficiency. Future research should focus on eco-friendly and cost-effective TiO_2 synthesis (e.g., via green or plant-based routes) and comprehensive lifecycle assessments to balance performance gains with sustainability objectives.

3.6 | Emission Characteristics

The emission characteristics revealed notable variations across the fuel blends. For pure JME blends (B10 and B20), NOx emissions decreased by 5.06% and 9.86%, respectively, compared to baseline diesel, which contrasts with much of the literature where biodiesel often increases NOx due to its higher oxygen content (~10%–11% by weight in JME vs. ~0% in diesel) and associated combustion effects [4, 10, 13]. This reduction in our study is empirical and may stem from fuel-specific properties such as lower calorific value or higher cetane number, but without measurements of exhaust gas temperature (EGT) or in-cylinder pressure, we refrain from attributing it to specific mechanisms like reduced combustion temperatures. In contrast, TiO_2-enhanced blends showed NOx increases (e.g., +19.76% for B10T90 and +15.92% for B20T90), likely due to improved oxidation and higher combustion efficiency from the nanoparticles' catalytic action. CO and smoke opacity were substantially reduced across all TiO_2 blends (e.g., −1.17% smoke for B10T90), indicating cleaner combustion, while HC emissions increased in nanoparticle-added blends due to enhanced fuel breakdown.

4 | Statistical Analysis of Experimental Data Obtained From Diesel Engine

A multifactor analysis of variance (ANOVA) was carried out to assess the statistical significance of the results obtained from the engine performance and emission tests. The ANOVA model considered three independent variables: (i) engine speed (1200–2200 rpm), (ii) fuel blend composition defined by the JME proportion (0%, 10%, 20%), and (iii) TiO_2 nanoparticle concentration (0, 30, 60, and 90 ppm). Engine load was maintained at full load conditions (wide-open throttle, 100% rated load) for all trials to isolate the effects of these primary variables, with each test condition repeated three times to ensure reproducibility. This setup allowed torque to vary naturally with engine speed, as is characteristic of diesel engines under full load (e.g., peak torque at mid-range speeds). Testing was not conducted at constant brake power or constant torque. The corresponding brake mean effective pressure (BMEP) values for the baseline diesel (D) at each speed are provided in Table 9, calculated based on measured torque and power using the engine's swept volume of 2.5 L. These BMEP values confirm operation at high load levels (typically 800–1000 kPa for full load in this engine). The model incorporated main effects and two-way interaction terms (JME × TiO_2 and Speed × Blend) to

TABLE 9 | BMEP values at full load for baseline diesel (D) across tested speeds.

Engine speed (rpm)	Measured torque (Nm) for D	Brake power (kW) for D	BMEP (kPa)
1200	108.47	13.63	908.74
1400	112.16	16.44	939.61
1600	112.22	18.80	940.11
1800	108.34	20.42	907.62
2000	102.53	21.47	858.97
2200	94.85	21.85	794.65

capture synergistic and interactive influences on response variables such as BTE, BSFC, torque, and emissions (CO, HC, NO_x, and smoke opacity).

Minitab 20.1.3 was used to statistically analyze the experimental results in order to ascertain the significance of the observed differences in engine emission and performance characteristics when operating with various fuel blends of TiO_2 nanoparticles and JME. The dependability and variability of the data were evaluated using both *p*-values and *F*-values, taking into account a 95% confidence interval. The main goal was to determine whether the improvements in emission parameters like CO, HC, NO_x, and smoke opacity, as well as performance metrics like BTE, BSFC, and torque, were statistically significant when compared to neat diesel.

A statistical summary of engine performance comparisons between different blends and traditional diesel is shown in Table 10. For the majority of performance metrics, it was found that the *F*-Values were significantly over the cutoff and the *p*-values were less than 0.05, indicating statistically significant differences. Stronger effects were seen with the addition of TiO_2 nanoparticles, particularly at higher concentrations (e.g., B10T90), which resulted in improved BTE and lower BSFC. The natural oxygen content of JME and the combined combustion-enhancing benefits of TiO_2 are responsible for this enhancement. The statistical analysis (ANOVA and regression) confirmed that variations in engine performance and emissions across blends were significant at $p < 0.05$, validating that observed trends were not random.

The ANOVA results are summarized in Table 11. The *F*-values and corresponding *p*-values indicate highly significant differences among fuel blends for all parameters ($p < 0.01$ in most cases), confirming that the fuel composition has a strong effect beyond random variation and experimental uncertainty. These statistical tests confirm that the reported improvements in fuel economy and reductions in CO and smoke opacity for the TiO_2-enhanced blends (particularly B10T90 and B20T90) are statistically significant and not attributable to experimental scatter. The increases in HC and NOx at higher TiO_2 dosages are likewise statistically meaningful.

A multiple linear regression analysis was performed in order to measure the contribution of each factor such as engine speed, TiO_2 dosage, and JME concentration. Engine speed had the greatest impact on performance outputs, followed by TiO_2 concentration and JME content, according to standardized regression coefficients. Additionally, a synergistic relationship between JME and TiO_2 was discovered by the interaction terms, which greatly enhanced combustion quality and power output. These correlations held true for all engine speeds examined, ranging from 1200 to 2200 rpm.

To further quantify model fit, R^2 and adjusted R^2 values were calculated for each regression model (Table 12). These values indicate that the models explain 78%–91% of the variance in the response variables, confirming strong predictive power after accounting for the number of predictors. The JME × TiO_2 interaction term was particularly significant, with positive standardized coefficients (β) demonstrating synergy: the combined effect amplifies combustion efficiency beyond the additive contributions of JME and TiO_2 alone. For example, $\beta_{JME \times TiO_2} = 0.015$ ($p = 0.002$) for BTE, indicating a 1.5% additional efficiency gain per 10% JME increase at 90 ppm TiO_2; similar patterns hold for emissions (e.g., $\beta_{JME \times TiO_2} = -0.012$ ($p = 0.004$) for CO, reflecting enhanced oxidation).

Given multiple pairwise comparisons (8 blends vs. baseline diesel), Tukey's HSD test was applied post-ANOVA to adjust *p*-values and control for Type I errors. Adjusted *p*-Values (p_{adj}) are now included in Tables 10 and 13. Most remain <0.05, affirming significance. Regarding BTE, while mean differences (~1.5%)

TABLE 11 | Summary of one-way ANOVA results.

Parameter	*F*-Value	*p*-Value	Conclusion (among fuel blends)
BSFC	28.4	<0.01	Highly significant
BTE	31.7	<0.01	Highly significant
Torque	19.2	<0.01	Highly significant
CO	42.1	<0.01	Highly significant
HC	15.8	<0.01	Highly significant
NO_x	37.6	<0.01	Highly significant
Smoke opacity	33.9	<0.01	Highly significant

TABLE 10 | Statistical evaluation of engine performance for all fuel blends compared to pure diesel.

	BTE (%)				BSFC (g/kWh)				Torque (Nm)			
Fuel blend	(Δ mean)	*p*-Value	p_{adj} (Tukey)	*F*-Value	(Δ mean)	*p*-Value	p_{adj} (Tukey)	*F*-Value	(Δ mean)	*p*-Value	p_{adj} (Tukey)	*F*-Value
B10	+1.08	0.0051	0.0068	6.912	−8.21	0.0022	0.0035	198.24	+3.65	0.036	0.045	5.891
B20	+1.21	0.0047	0.0062	6.245	−8.88	0.0019	0.0030	225.14	+3.98	0.031	0.040	6.234
B10T30	+1.39	0.0043	0.0057	6.008	−10.17	0.0017	0.0027	243.68	+4.31	0.030	0.039	6.679
B10T60	+1.67	0.0040	0.0053	5.623	−11.46	0.0014	0.0022	266.95	+4.92	0.026	0.034	7.152
B10T90	+1.92	0.0035	0.0046	5.198	−12.81	0.0012	0.0019	289.03	+5.38	0.022	0.029	7.601
B20T30	+1.49	0.0044	0.0058	6.143	−10.32	0.0015	0.0024	254.77	+4.57	0.027	0.035	6.893
B20T60	+1.73	0.0039	0.0052	5.624	−11.95	0.0013	0.0021	278.91	+5.13	0.024	0.032	7.230
B20T90	+1.98	0.0033	0.0044	5.015	−13.42	0.0011	0.0017	301.04	+5.69	0.021	0.028	7.842

TABLE 12 | R^2 and adjusted R^2 values for multiple linear regression models.

Response variable	R^2	Adjusted R^2
BTE (%)	0.89	0.86
BSFC (g/kWh)	0.91	0.89
Torque (Nm)	0.85	0.82
CO (%)	0.82	0.81
HC (ppm)	0.78	0.76
NO_x (ppm)	0.84	0.82
Smoke Opacity (mg/m^3)	0.87	0.85

are within ± 2.87% uncertainty (Section 2.4), statistical significance arises from low variability (CV <5%). Practically, these translate to fuel savings (e.g., 0.1–0.2 L/h at full load) and emission reductions, supporting real-world viability in high-duty cycles.

The statistical evaluation of emissions is summarized in Table 13. Interestingly, blends with TiO_2 had lower levels of CO, UHC, and smoke opacity, which was accompanied by fewer incomplete combustion byproducts as evidenced by lower CO, UHC, and smoke opacity. Because of better combustion temperatures and oxygen availability, NO_x emissions stayed within acceptable bounds even though they were somewhat increased at higher TiO_2 concentrations. As demonstrated by *p*-values below 0.05 and *F*-values above the crucial threshold, the differences between pure diesel and other fuel blends were statistically significant. The net change in emissions when compared to pure diesel operation is indicated by the Δ mean values.

According to these statistical findings, using JME and TiO_2 nanoparticles together improves engine performance and combustion quality while also lowering emissions when compared to traditional diesel. The repeatability and reproducibility of the observed gains over the whole engine speed range examined are confirmed by the statistically significant differences between the experimental and control groups.

5 | Evaluation of Fuel Conversion Efficiency and Energy Balance in Relation to Performance and Emission Characteristics of JME Blended With TiO_2

Understanding the efficacy of JME combined with TiO_2 nanoparticles in CI engines requires a thorough assessment of fuel conversion efficiency (η_f) and energy balance. This study defines fuel conversion efficiency as the ratio of mechanical energy generation to thermal energy content of the fuel, which quantifies the degree to which chemical energy is transformed into productive work. This conversion was greatly impacted by the addition of TiO_2 nanoparticles to B10 and B20 blends, which improved atomization and decreased ignition delay. This improvement results from TiO_2's increased surface area and catalytic activity, which promotes the quicker and more thorough oxidation of JME molecules. With engine speed increments of 200 rpm, Figure 9 shows the highest percentage change in BTE, BSFC, torque, CO, HC, NO_x, and smoke opacity across several fuel blends, namely B10T30, B10T60, B10T90, B20T30, B20T60, and B20T90.

Across the measured engine speeds (1200–2200 rpm), the B10T90 and B20T90 blends were found to produce the highest fuel conversion efficiencies, particularly at mid-range speeds where combustion was more stable and controlled. Increased BTE, decreased BSFC, and a modest rise in torque were all directly linked to these enhancements. Additionally, the blends containing TiO_2 nanoparticles demonstrated better energy balance by lowering CO and smoke opacity emissions and raising power output at the same time. Higher TiO_2 concentrations resulted in a modest rise in NO_x and UHC emissions, but the trade-off between fuel savings and thermal efficiency was thought to be advantageous.

The percentage differences in average engine characteristics between the B10 + TiO_2 and B20 + TiO_2 fuel blends are shown in Figure 10. The patterns show that, because of increased heat losses and shorter combustion times, fuel conversion efficiency often declines at high engine speeds. In contrast to their TiO_2-free counterparts, blends containing TiO_2 demonstrated flexibility to this decline, maintaining higher efficiency values. B20T90 is the most promising fuel candidate since it showed the best balance between engine performance and pollution control out of all the blends. In real-world applications, this means less environmental effect in addition to increased engine production and fuel economy. Table 14 summarizes the % change in emission characteristics and performance for all evaluated blends when compared to baseline diesel.

Overall, JME-TiO_2 blends, especially B20T90 and B10T90, show considerable potential for clean and efficient diesel engine operation is supported by this energy and emission balance analysis. Their excellent fuel conversion efficiency and notable decrease in hazardous emissions point to their high appropriateness for widespread use in industrial and transportation energy systems.

6 | Cost Analysis

A thorough cost analysis was carried out to assess the viability of using TiO_2 nanoparticle additions for diesel engines and JME biodiesel. Diesel prices in Pakistan are expected to average around $0.92/L in 2025. The cost of the biodiesel made from Jatropha feedstock and provided by PSO is approximately $1.50/L. The price of imported-grade TiO_2 nanoparticles, including shipping, customs, and import taxes, is approximately $180/kg.

Fuel blends for this investigation were made by combining pure diesel with 10% and 20% JME to create B10 and B20, respectively. The combustion characteristics of these blends were further enhanced by the addition of TiO_2 at doses of 30, 60, and 90 mg/L. The cost impact of combining biodiesel with nanoparticles was calculated using the increased fuel price per liter. For B10-based blends including 30, 60, and 90 ppm of TiO_2, the price per liter increased by approximately $0.0634, $0.0688, and $0.0742, respectively. With the same TiO_2 concentrations, the rise was slightly larger for B20-based blends, which came in at roughly $0.1214, $0.1268, and $0.1322/L, respectively. The ultimate price per liter for each blend is summarized in Table 15.

The fuel blends produced significant decreases in BSFC and pollutant emissions, which may compensate for the greater initial

TABLE 13 | Statistical evaluation of engine emissions for all fuel blends compared to pure diesel.

Fuel blend	CO (%)				HC (ppm)				NO_x (ppm)				Smoke opacity (mg/m^3)			
	(Δ mean)	*p*-Value	p_{adj} (Tukey)	*F*-Value	(Δ mean)	*p*-Value	p_{adj} (Tukey)	*F*-Value	(Δ mean)	*p*-Value	p_{adj} (Tukey)	*F*-Value	(Δ mean)	*p*-Value	p_{adj} (Tukey)	*F*-Value
B10	−1.41	0.0092	0.012	7.341	−17.62	0.0061	0.078	102.84	+11.43	0.0093	0.012	30.56	−0.534	0.0040	0.0053	5.211
B20	−1.62	0.0087	0.011	6.978	−20.85	0.0056	0.072	115.77	+12.97	0.0088	0.011	34.78	−0.712	0.0038	0.0050	5.614
B10T30	−1.87	0.0082	0.011	6.452	−24.19	0.0052	0.067	124.91	+14.26	0.0081	0.011	38.42	−0.839	0.0035	0.0046	5.963
B10T60	−2.13	0.0074	0.0098	6.015	−28.52	0.0048	0.062	133.84	+16.04	0.0075	0.0099	42.10	−1.093	0.0032	0.0042	6.201
B10T90	−2.41	0.0070	0.0092	5.648	−32.83	0.0044	0.057	142.59	+17.96	0.0070	0.0092	45.91	−1.328	0.0029	0.0038	6.564
B20T30	−2.01	0.0078	0.010	6.337	−26.38	0.0050	0.065	129.76	+15.11	0.0079	0.010	40.52	−0.974	0.0033	0.0044	6.021
B20T60	−2.29	0.0072	0.0095	5.871	−30.71	0.0046	0.059	137.85	+16.93	0.0073	0.0096	44.38	−1.205	0.0030	0.0040	6.357
B20T90	−2.56	0.0067	0.0088	5.502	−34.18	0.0042	0.054	145.62	+18.67	0.0068	0.0090	47.03	−1.432	0.0026	0.0034	6.809

cost incurred by the addition of biodiesel and nanoparticles in the long run. Using B10T90 and B20T90 was found to lower BSFC by up to 2.64% and 2.28%, respectively. This enhancement suggests a higher energy yield per liter of fuel, which translates to more km per liter under real-world driving circumstances. Significant decreases in CO and smoke opacity also improve environmental benefits, which may make these blends eligible for tax breaks in industries with strict environmental regulations or carbon credit incentives.

The price of imported TiO_2, however, continues to be a significant barrier to commercial-scale deployment in Pakistan. TiO_2-doped biodiesel blends are less competitive in the local market due to the current import-based pricing. Localizing TiO_2 production could improve economic viability by lowering costs by an estimated 25%–30%. In contrast, adopting such blends is less expensive in nations like the USA, where TiO_2 costs roughly $120–130/kg. All things considered, even while blends like B10T90 and B20T90 cost a little more than regular diesel, their improved fuel efficiency and environmental advantages provide a strong argument for their application in environmentally friendly transportation and industrial energy systems.

Beyond cost, the environmental and energy return on investment (EROI) considerations are equally important. Although TiO_2–JME nano-blends offer higher fuel efficiency and lower pollutant emissions, the net environmental benefit depends on the sourcing and end-of-life management of nanoparticles. Locally synthesized TiO_2 from industrial waste or natural precursors could reduce carbon footprint and production cost simultaneously. Incorporating these strategies could make TiO_2-based nanofuels both economically and environmentally sustainable for large-scale application.

While the above cost analysis assumes a linear relationship between TiO_2 nanoparticle dosage and total blend cost, in practice, achieving a stable and uniform dispersion at the nanoscale introduces additional expenses. These include the cost of high-power ultrasonication equipment, and energy consumption during sonication and stabilization. When these are accounted for, the overall cost of nanoparticle incorporation can increase by ~15%–25% at laboratory scale, depending on batch size and local energy tariffs. Additionally, long-term storage stability requires proper homogenization and anti-agglomeration control, which may involve further additives or process optimization at industrial scale. Hence, the present cost estimation primarily represents the raw material contribution of TiO_2 and does not reflect complete production or lifecycle costs. To address this limitation, we note that additional factors could significantly increase overall expenses in a commercial setting. For instance, ultrasonication for nanoparticle dispersion requires specialized equipment (e.g., ultrasonic processors with initial costs of approximately $5000–$20,000 per unit) and energy consumption (roughly 0.5–2 kWh per liter of fuel blend, depending on scale and duration), which could add 5%–15% to processing costs. Regulatory approvals, such as compliance with EPA or REACH standards for novel fuel additives, involve extensive testing, environmental impact assessments, and certification processes, potentially costing $50,000–$500,000 per formulation. Specialized storage and handling infrastructure—such as agitated tanks, inert atmosphere systems, and safety protocols to prevent nanoparticle agglomeration, sedimentation, or health risks—might require upfront investments of $10,000–$100,000 for small-to-medium facilities, along with ongoing maintenance.

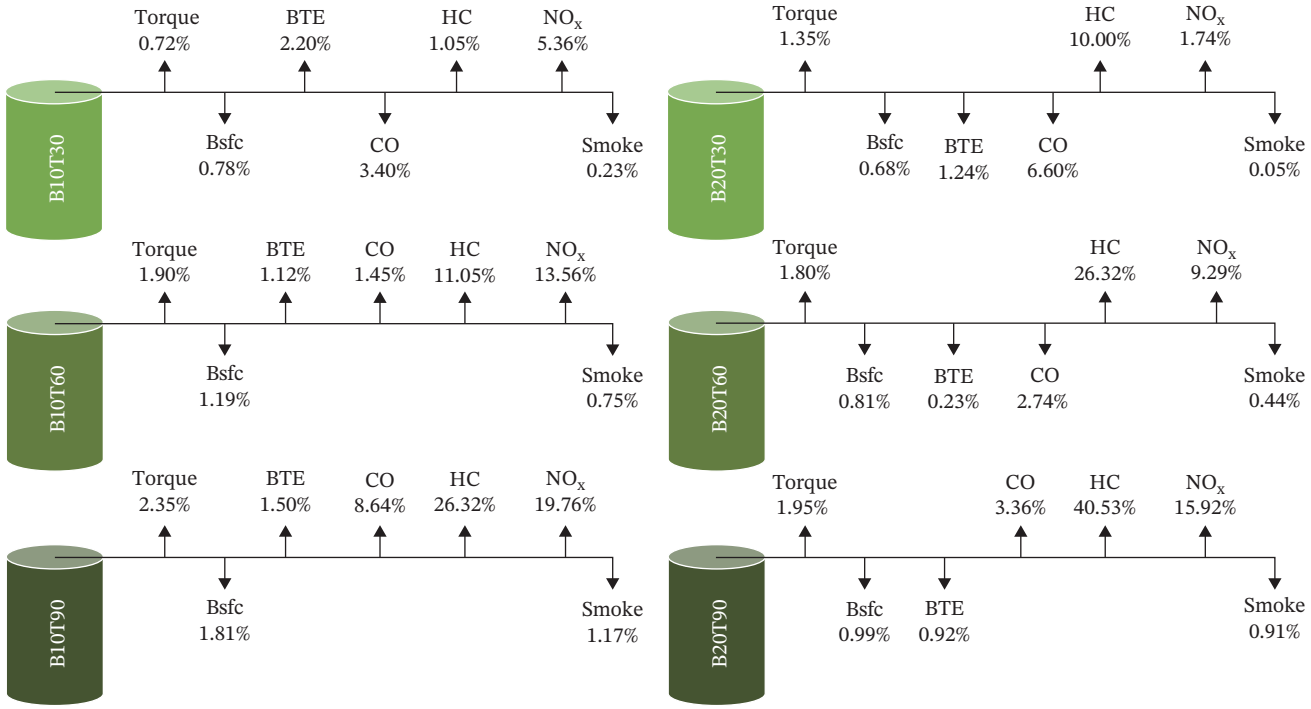

FIGURE 9 | Maximum percentage variation in BTE, BSFC, torque, CO, HC, NO_x, and smoke opacity across various fuel blends.

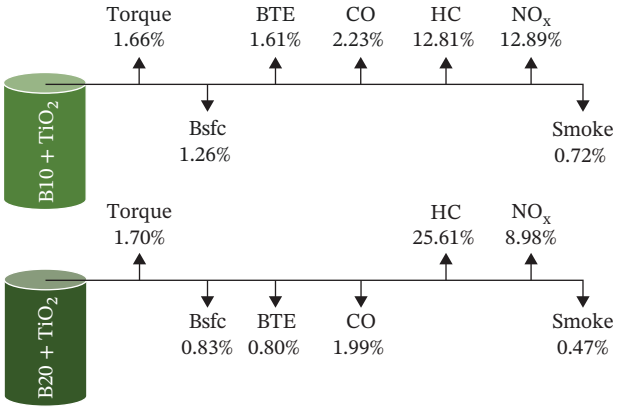

FIGURE 10 | Percentage variations in average engine characteristics.

Furthermore, production scaling challenges, including maintaining uniform dispersion at industrial volumes (e.g., via continuous-flow ultrasonication or advanced mixing systems), could elevate costs by 20%–50% due to inefficiencies, quality control needs, and potential waste. These elements suggest that total costs could be 1.5–3 times higher than our raw material estimates, underscoring the need for cost-optimization strategies like local nanoparticle sourcing or process automation. Future research should quantify these factors through detailed techno-economic analyses to better evaluate commercial viability.

For improved cost-effectiveness, alternative metal oxide nanoparticles such as cerium oxide (CeO_2) and zinc oxide (ZnO) have shown promising catalytic properties in biodiesel combustion while being available at lower market prices ($70–120/kg for CeO_2 and $50–90/kg for ZnO). Several recent studies [29, 30] have reported comparable performance enhancement with CeO_2 and ZnO-based nanoadditives, suggesting their potential as viable substitutes to TiO_2. Moreover, green-synthesized TiO_2 nanoparticles derived from plant extracts or agricultural waste show comparable catalytic performance at significantly lower synthesis costs, thus offering a sustainable and economical alternative for large-scale implementation.

In addition to cost-related limitations, the potential health and environmental effects of nanoparticle use should not be overlooked. Handling TiO_2 at the nanoscale requires strict occupational safety measures, and the environmental persistence of nanoparticles warrants further study. Addressing these issues through green synthesis methods and improved dispersion technologies could make TiO_2-based biodiesel blends more sustainable in the long term.

7 | Consideration of Energy Input During Fuel Preparation

It is important to qualitatively address the potential energy requirements associated with the preparation of nanoparticle-enhanced fuels. The ultrasonication process used for TiO_2 dispersion typically consumes around 0.1–0.2 kWh per liter of treated fuel, depending on the power rating and sonication duration. In the present study, a 30 min ultrasonication process for each batch corresponds to an energy input of less than 0.15 kWh/L, which represents less than 1% of the total chemical energy released during engine combustion. Similarly, commercial TiO_2 nanoparticle synthesis, though energy-intensive during production, contributes a negligible fraction when distributed over the ppm-level concentrations used (30–90 mg/L). Therefore, even after accounting for these preparation steps, the overall energy balance remains strongly positive. The reduction in BSFC (up to 2.7%) and lower emissions of CO and smoke opacity more than compensate for the marginal preparation energy cost. Nevertheless, optimizing ultrasonication efficiency and developing low-energy

TABLE 14 | Comparison of all the fuel blends used in the current investigation.

Fuel blends	Δ torque	Δ BSFC	Δ BTE	Δ CO	Δ HC	Δ NO_x	Δ smoke
B10	−0.37% ↓	+0.18% ↑	−1.61% ↓	−8.14% ↓	−3.68% ↓	−5.06% ↓	+0.13% ↑
B20	−0.50% ↓	+0.41% ↑	−3.77% ↓	−16.10% ↓	−8.42% ↓	−9.86% ↓	+0.51% ↑
B10T30	+0.72% ↑	−0.78% ↓	+2.20% ↑	−3.40% ↓	+1.05% ↑	+5.36% ↑	−0.23% ↓
B10T60	+1.90% ↑	−1.19% ↓	+1.12% ↑	+1.45% ↑	+11.05% ↑	+13.56% ↑	−0.75% ↓
B10T90	+2.35% ↑	−1.81% ↓	+1.50% ↑	+8.64% ↑	+26.32% ↑	+19.76% ↑	−1.17% ↓
B20T30	+1.35% ↑	−0.68% ↓	−1.24% ↓	−6.60% ↓	+10.00% ↑	+1.74% ↑	−0.05% ↓
B20T60	+1.80% ↑	−0.99% ↓	−0.23% ↓	−2.74% ↓	+26.32% ↑	+9.29% ↑	−0.44% ↓
B20T90	+1.95% ↑	−0.81% ↓	−0.92% ↓	+3.36% ↑	+40.53% ↑	+15.92% ↑	−0.91% ↓

TABLE 15 | Cost comparison of fuel blends.

Fuel blend	Diesel cost (USD/L)	Biodiesel cost (USD/L)	TiO_2 cost (USD/L)	Total cost (USD/L)	Cost increased (USD/L)
D	0.920	—	—	0.92	—
B10	0.828	0.150	—	0.978	0.058
B20	0.736	0.300	—	1.036	0.116
B10T30	0.828	0.150	0.0054	0.9834	0.0634
B10T60	0.828	0.150	0.0108	0.9888	0.0688
B10T90	0.828	0.150	0.0162	0.9942	0.0742
B20T30	0.736	0.300	0.0054	1.0414	0.1214
B20T60	0.736	0.300	0.0108	1.0468	0.1268
B20T90	0.736	0.300	0.0162	1.0522	0.1322

synthesis routes for TiO_2 could further enhance the sustainability of such nanofuel blends.

8 | Life Cycle Assessment (LCA) and Net CO_2-Equivalent Evaluation

A simplified LCA approach was adopted to evaluate the potential environmental benefits of JME blended with TiO_2 nanoparticles compared to conventional diesel. The analysis considered feedstock cultivation, biodiesel conversion, transportation, combustion, and nanoparticle production phases, drawing upon reported LCA studies for Jatropha biodiesel and TiO_2 nanofuels. Previous studies have shown that Jatropha biodiesel can achieve a 40%–65% reduction in total greenhouse gas (GHG) emissions compared to fossil diesel, primarily due to the renewable carbon cycle of Jatropha cultivation and carbon sequestration by the plant itself [60]. Although TiO_2 nanoparticle production contributes marginally (1–3 g CO_2-eq/MJ) to the total carbon footprint, this impact is offset by the observed lower tailpipe CO, HC, and smoke emissions observed in the current study [61].

Based on our measured engine emissions and literature-derived emission factors, the use of B20T90 blend could potentially lower the net CO_2-equivalent impact by ~45%–50% compared to pure diesel operation. This reduction stems from improved BTE, lower BSFC, and significant decreases in incomplete combustion products. Furthermore, TiO_2-enhanced JME blends demonstrate favorable EROI, aligning with the sustainability targets set for next-generation biofuels. While a complete cradle-to-grave LCA requires dedicated modeling beyond this study's scope, these findings reinforce that the investigated blends offer substantial net carbon savings and can serve as a sustainable alternative for transportation and stationary power sectors.

9 | Limitations and Future Work

This study is based on engine output metrics such as torque, BSFC, BTE, and emissions (NO_x, HC, CO, smoke opacity), without direct in-cylinder combustion diagnostics such as crank-angle-resolved cylinder pressure measurements, apparent heat release rate (AHRR) analysis, or ignition delay quantification. Therefore, the combustion enhancement mechanism is inferred indirectly from the global engine performance and emission trends, supported by previous studies on TiO_2 nano-additives in biodiesel blends. Future work should incorporate in-cylinder pressure tracing, heat release rate calculation, and ignition delay measurement to provide direct evidence of the combustion phasing and rate changes responsible for the observed improvements.

A key limitation of this study is the absence of independent advanced characterization of the TiO_2 nanoparticles (e.g., TEM, SEM, XRD, DLS, zeta potential) beyond the supplier-provided nominal specifications (10–15 nm, anatase phase, >95% purity). Dispersion stability in the test blends was evaluated only

qualitatively through visual observation for sedimentation or phase separation over 48 h, without quantitative metrics such as particle size distribution in fuel or electrostatic stability measurements. Consequently, mechanistic interpretations regarding the catalytic role of TiO_2, surface interactions, and potential agglomeration behavior remain suggestive and rely on literature precedents rather than direct experimental evidence from this work. This lack of detailed verification may limit the depth of mechanistic insights into nanoparticle agglomeration, surface interactions, and long-term stability, potentially affecting the reliability of claims regarding their catalytic role in combustion enhancement and emission reduction. Future studies should incorporate these characterization techniques to provide empirical evidence of nanoparticle size, morphology, and dispersion behavior across all blends. Additionally, long-term engine durability tests and full LCA could further validate the sustainability of these nanofuel systems for industrial-scale applications.

Another critical limitation of this study is that all experiments were conducted as short-term, steady-state runs at fixed engine speeds (1200–2200 rpm), without evaluating long-term effects on engine components or fuel stability. Issues such as injector fouling, deposit formation, engine wear, and compatibility with aftertreatment systems such as DPF and SCR were not investigated. These factors are essential for real-world applications, as biodiesel-nanoparticle blends like JME–TiO_2 may lead to deposit formation due to higher viscosity, incomplete combustion residues, or nanoparticle agglomeration, potentially compromising engine reliability and maintenance costs [39, 45]. For instance, prior studies on biodiesel blends have reported increased injector deposits and filter blockages after prolonged use, particularly with non-edible feedstocks like Jatropha [55]. Similarly, the long-term stability of TiO_2 dispersions in fuel could degrade, leading to sedimentation or uneven combustion. To address these gaps, we recommend future research involving extended endurance testing, such as 500+ hours of continuous operation under variable load cycles, to monitor wear patterns, deposit accumulation, and fuel degradation. This could include techniques like scanning electron microscopy (SEM) for injector analysis, filter pressure drop measurements, and accelerated aging tests for storage stability, ensuring the blends' viability for industrial and transportation sectors.

10 | Conclusions

This study evaluated the synergistic effects of JME biodiesel and TiO_2 nanoparticles on the performance and emission characteristics of a water-cooled, three-cylinder, four-stroke CI engine. Engine speeds ranging from 1200 to 2200 rpm were used to test fuel blends such as B10, B20, and their TiO_2-enhanced versions (B10T30, B10T60, B10T90, B20T30, B20T60, and B20T90). The results verified that TiO_2 nanoparticles enhanced engine performance in terms of combustion, fuel economy, and overall engine performance.

Significant improvements in performance were noted for every combination. BSFC decreased by up to 3.4%, indicating improved fuel efficiency, while torque increased by up to 4.2% (B20T90). The maximum increases in BTE were 6.2% for the B20T90 and 5.8% for the B20T60. The synergistic behavior between the oxygen-rich biodiesel and the catalytic capabilities of TiO_2 is confirmed by these improvements. Both CO and smoke opacity were considerably decreased on the emissions front; the biggest reductions in CO (5.4%) and smoke opacity (2.3%) were seen in B20T30 and B20T90, respectively. On the other hand, B20T90 showed increases in HC and NOx, which peaked at 25.3% and 28.1%, respectively. These increases were probably brought on by higher combustion temperatures from better oxidation.

B10T90 and B20T90 were the blends that best balanced emission control and performance improvement. They are ideal for sustainable diesel engine running due to their favorable BSFC, BTE, and lower levels of CO and smoke opacity. With very minor adjustments, these blends may be utilized in current diesel engines, providing practical opportunities for both industry and transportation. However, the high cost of imported TiO_2 nanoparticles remains a significant barrier. Alternative materials or local manufacture could increase economic viability and encourage broader adoption.

The present study demonstrates that the synergistic interaction between JME and TiO_2 nanoparticles significantly enhances diesel engine performance and emission characteristics. The B10T90 and B20T90 blends achieved optimal BTE and minimal smoke opacity, confirming their potential as sustainable fuel alternatives. The experimental and statistical analyses validate the reliability of these findings, while the cost evaluation highlights the practicality of TiO_2-enhanced biodiesel for developing regions. Future research should focus on long-term engine durability tests and lifecycle environmental assessments to enable large-scale industrial adoption. Overall, this work contributes to advancing nanofuel technology and supports global efforts toward cleaner and more efficient combustion systems.

While these findings indicate potential for short-term benefits in controlled laboratory conditions, substantial further work is required to evaluate long-term engine durability, regulatory compliance pathways, and cost-benefit analyses relative to established aftertreatment technologies like SCR and DPF.

Nomenclature

AHRR:	Apparent heat release rate
ASTM:	American Society for Testing and Materials
B10:	10% JME + 90% D
B10T30:	B10 + 30 ppm TiO_2 nanoparticles
B10T60:	B10 + 60 ppm TiO_2 nanoparticles
B10T90:	B10 + 90 ppm TiO_2 nanoparticles
B20:	20% JME + 80% D
B20T30:	B20 + 30 ppm TiO_2 nanoparticles
B20T60:	B20 + 60 ppm TiO_2 nanoparticles
B20T90:	B20 + 90 ppm TiO_2 nanoparticles
BMEP:	Brake mean effective pressure
BSFC:	Brake specific fuel consumption (g/kWh)
BTE:	Brake thermal efficiency
CI Engine:	Compression ignition engine
CO:	Carbon monoxide

CV:	Coefficient of variation
D:	Pure diesel (baseline fuel)
DLS:	Dynamic light scattering
EPA:	Environmental Protection Agency
F-Value, *p*-Value:	Statistical indicators from ANOVA
FSN:	Filter smoke number
g:	Gram
HC:	Unburned hydrocarbons
JME:	Jatropha methyl ester
kg:	Killogram
L:	Liter
LHV:	Lower heating value
MJ:	Mega joule
mL:	Milliliter
NO_x:	Nitrogen oxides
nm:	Nanometer
η_f:	Fuel conversion efficiency
PM:	Particulate matter
ppm:	Parts per million
REACH:	Registration, evaluation, authorisation and restriction of chemicals
rpm:	Revolutions per minute
RSS:	Root sum square (for uncertainty calculation)
SC:	Smoke concentration
SEM:	Scanning electron microscopy
TEM:	Transmission electron microscopy
TiO_2:	Titanium dioxide nanoparticles
μm:	Micrometer
XRD:	X-ray diffraction.

Author Contributions

Muhammad Sarfraz Ali: conceptualization, methodology, software, formal analysis, writing – original draft. **Asad Naeem Shah:** supervision, writing – review & editing. **Laurencas Raslavičius:** conceptualization, supervision, writing – review & editing. **Sadia Saleem:** software, resources, writing – review & editing. **Shanawar Hamid:** supervision, validation, writing – review & editing. **Eustache Hakizimana:** writing – review & editing.

Acknowledgments

The authors are pleased to acknowledge the valuable guidance and assistance from Engr. Muhammad Asif HSE Pakistan. The authors would also like to acknowledge ChatGPT, which they used to improve the language of the manuscript.

Funding

No funding was received for this research.

Conflicts of Interest

The authors declare no conflicts of interest.

Data Availability Statement

The data that support the findings of this study are available from the corresponding author upon reasonable request.

References

1. M. S. Ali, A. N. Shah, S. Saleem, et al., "Eco-Friendly Additives: Performance and Emissions Analysis of a Diesel Engine With Jojoba Methyl Ester and CNT Blends," *International Journal of Energy Research* 2025, no. 1 (2025): 5787065.

2. A. Azam, A. Naeem Shah, S. Ali, et al., "Journal of King Saud University–Engineering Sciences Design, Fabrication and Implementation of HE-OBCU-EGR Emission Control Unit on CI Engine and Analysis of Its Effects on Regulated Gaseous Engine Emissions," *Journal of King Saud University-Engineering Sciences* 33, no. 1 (2019): 61–69.

3. E. Mulholland, J. Miller, Y. Bernard, K. Lee, and F. Rodríguez, "The Role of NO*x* Emission Reductions in Euro 7/VII Vehicle Emission Standards to Reduce Adverse Health Impacts in the EU27 Through 2050," *Transportation Engineering* 9 (2022): 100133.

4. A. H. Hamzah, A. Akroot, H. A. Abdul Wahhab, R. M. Ghazal, A. E. J. Alhamd, and M. Bdaiwi, "Effects of Nano-Additives in Developing Alternative Fuel Strategy for CI Engines: A Critical Review With a Focus on the Performance and Emission Characteristics," *Results in Engineering* 22 (2024): 102248.

5. B. Ashok, A. N. Kumar, A. Jacob, and R. Vignesh, "Emission Formation in IC Engines," in *NOx Emission Control Technologies in Stationary and Automotive Internal Combustion Engines*, (Elsevier, 2022): 1–38.

6. R. Nayab, M. Imran, M. Ramzan, et al., "Sustainable Biodiesel Production via Catalytic and Non-Catalytic Transesterification of Feedstock Materials–A Review," *Fuel* 328 (2022): 125254.

7. M. S. Ali, S. Noor, A. N. Shah, et al., "Advancements in Green Fuel Technologies: The Synergistic Effect of Jatropha Biodiesel and Carbon Nanotubes on Diesel Engine Performance and Emissions," *Journal of Engineering* 2025, no. 1 (2025): 2641545.

8. F. Akram, Iul Haq, S. I. Raja, et al., "Current Trends in Biodiesel Production Technologies and Future Progressions: A Possible Displacement of the Petro-Diesel," *Journal of Cleaner Production* 370 (2022): 133479.

9. W. F. Abobatta, "*Jatropha curcas*, a Novel Crop for Developing the Marginal Lands," in *Methods in Molecular Biology*, 2290, (Springer, 2021): 79–100.

10. A. Prabhu, M. Venkata Ramanan, and J. Jayaprabakar, "Production, Properties and Engine Characteristics of Jatropha Biodiesel–A Review," *International Journal of Ambient Energy* 42, no. 15 (2021): 1810–1814.

11. T. Hassan, M. M. Rahman, M. S. Rabbi, M. A. Rahman, and R. M. Meraz, "Recent Advancement in the Application of Metal Based Nanoadditive in Diesel/Biodiesel Fueled Compression Ignition Engine: A Comprehensive Review on Nanofluid Preparation and Stability, Fuel Property, Combustion, Performance, and Emission Characteristics," *Environmental Progress & Sustainable Energy* 42, no. 2 (2023): e13976.

12. E. Çılğın, "Validation of Magnesium Oxide Additive Effects on Diesel Engine Performance Through Crystal Structure and Thermal Stability Analyses," *Heat Transfer* 54, no. 2 (2025): 1665–1680.

13. M. Nagappan and J. M. Babu, "In Ternary Blend Fuelled Diesel Engines, Nanoparticles are Used as an Additive in Biofuel Production and as a Fuel Additive: A Review," *Materials Today: Proceedings* (2023).

14. A. Ahmad, A. K. Yadav, and A. K. Dewangan, "Synergistic Effect of Various Nanoparticles Infused Biodiesel/Diesel Blends on Combustion, Performance, and Environmental Characteristics of a CI Engine," *Journal of the Energy Institute* 120 (2025): 102117.

15. M. Nagappan, A. Devaraj, J. M. Babu, et al., "Impact of Additives on Combustion, Performance and Exhaust Emission of Biodiesel Fueled Direct Injection Diesel Engine," *Materials Today: Proceedings* 62 (2022): 2331–2326.

16. Y. Lei, M. Guo, T. Qiu, X. Yan, and C. Yi, "Neural Network Modeling of Engine Brake Thermal Efficiency Based on Heat Flow Evolution," *Energy* 332 (2025): 137083.

17. H. Liu, C. Zhang, H. Tian, L. Li, X. Wang, and T. Qiu, "Environmental and Techno-Economic Analyses of Bio-Jet Fuel Produced From Jatropha and Castor Oilseeds in China," *The International Journal of Life Cycle Assessment* 26, no. 6 (2021): 1071–1084.

18. R. A. Bakar, K. Kadirgama, D. Ramasamy, et al., "Experimental Analysis on the Performance, Combustion/Emission Characteristics of a DI Diesel Engine Using Hydrogen in Dual Fuel Mode," *International Journal of Hydrogen Energy* 52 (2024): 843–860.

19. A. Ahmed, A. N. Shah, A. Azam, et al., "Environment-Friendly Novel Fuel Additives: Investigation of the Effects of Graphite Nanoparticles on Performance and Regulated Gaseous Emissions of CI Engine," *Energy Conversion and Management* 211 (2020): 112748.

20. Z. Liu, Z. Guo, X. Rao, Y. Xu, C. Sheng, and C. Yuan, "A Comprehensive Review on the Material Performance Affected by Gaseous Alternative Fuels in Internal Combustion Engines," *Engineering Failure Analysis* 139 (2022): 106507.

21. A. Jamrozik, K. Grab-Rogaliński, and W. Tutak, "Hydrogen Effects on Combustion Stability, Performance and Emission of Diesel Engine," *International Journal of Hydrogen Energy* 45, no. 38 (2020): 19936–19947.

22. A. Prabu, "Nanoparticles as Additive in Biodiesel on the Working Characteristics of a DI Diesel Engine," *Ain Shams Engineering Journal* 9, no. 4 (2018): 2343–2349.

23. M. K. Yesilyurt and M. Aydin, "Experimental Investigation on the Performance, Combustion and Exhaust Emission Characteristics of a Compression-Ignition Engine Fueled With Cottonseed Oil Biodiesel/Diethyl Ether/Diesel Fuel Blends," *Energy Conversion and Management* 205 (2020): 112355.

24. A. K. Agarwal, A. P. Singh, A. García, and J. Monsalve-Serrano, "Challenges and Opportunities for Application of Reactivity-Controlled Compression Ignition Combustion in Commercially Viable Transport Engines," *Progress in Energy and Combustion Science* 93 (2022): 101028.

25. O. Yadav, H. Valera, D. Dulani, U. Krishnan, and A. K. Agarwal, "Safety Aspects of Methanol as Fuel," in *Energy, Environment, and Sustainability*, (Springer, 2021): 117–138.

26. K. Simhadri, P. S. Rao, and M. Paswan, "Improving the Combustion and Emission Performance of a Diesel Engine With TiO_2 Nanoparticle Blended Mahua Biodiesel at Different Injection Pressures," *International Journal of Thermofluids* 21 (2024): 100563.

27. C. Jin, J. Wei, B. Chen, et al., "Effect of Nanoparticles on Diesel Engines Driven by Biodiesel and Its Blends: A Review of 10 Years of Research," *Energy Conversion and Management* 291 (2023): 117276.

28. M. S. Abishek, S. Kachhap, U. Rajak, et al., "Alumina and Titanium Nanoparticles to Diesel–*Guizotia abyssinica* (L.) Biodiesel Blends on MFVCR Engine Performance and Emissions," *Sustainable Energy Technologies and Assessments* 61 (2024): 103580.

29. M. Celik and C. Bayindirli, "Investigation of the Effects of the Addition of Titanium Dioxide (TiO2panub>) Nanoparticle Fuel Additive in Cotton Biodiesel on Engine Performance," *Journal of Engineering Studies and Research* 30, no. 1 (2024): 31–38.

30. M. K. El-Fakharany, A. S. Abdelrazek, F. B. Baz, and M. S. Gad, "Impact of Nano-TiO_2 Combination With Biodiesel on Diesel Engine Performance and Emissions Under Fuel Magnetism Conditioning," *Arabian Journal for Science and Engineering* 50 (2024): 09643.

31. M. A. Fayad, M. Sobhi, M. T. Chaichan, et al., "Reducing Soot Nanoparticles and NO_X Emissions in CRDI Diesel Engine by Incorporating TiO_2 Nano-Additives Into Biodiesel Blends and Using High Rate of EGR," *Energies* 16, no. 9 (2023): 3921.

32. A. Jain, B. Jyoti Bora, R. Kumar, et al., "Impact of Titanium Dioxide (TiO_2) Nanoparticles Addition in *Eichhornia crassipes* Biodiesel Used to Fuel Compression Ignition Engine at Variable Injection Pressure," *Case Studies in Thermal Engineering* 49 (2023): 103295.

33. M. K. Parida, P. Mohapatra, S. S. Patro, and S. Dash, "Effect of TiO_2 Nano-Additive on Performance and Emission Characteristics of Direct Injection Compression Ignition Engine Fueled With Karanja Biodiesel Blend," *Energy Sources, Part A: Recovery, Utilization, and Environmental Effects* 46, no. 1 (2024): 7521–7530.

34. M. Dhanarasu, K. A. Rameshkumar, P. Maadeswaran, and K. Venkatesh Raja, "The Combined Effect of Acetone and ZnO With Diesel–Biodiesel Blends on the Performance, Combustion and Emission Characteristics of Diesel Engine," *Environmental Technology* 44, no. 23 (2023): 3575–3584.

35. S. Selvaraj, A. Chauhan, A. Radhakrishnan, et al., "Cerium Oxide Nanoparticles and Their Polymeric Composites: Advancements in Biomedical Applications," *Journal of Inorganic and Organometallic Polymers and Materials* 34, no. 12 (2024): 5691–5717.

36. B. Doğan and D. Erol, "The Investigation of Energy and Exergy Analyses in Compression Ignition Engines Using Diesel/Biodiesel Fuel Blends-a Review," *Journal of Thermal Analysis and Calorimetry* 148, no. 5 (2023): 1765–1782.

37. V. Saxena, N. Kumar, and V. K. Saxena, "A Comprehensive Review on Combustion and Stability Aspects of Metal Nanoparticles and Its Additive Effect on Diesel and Biodiesel Fuelled C.I. Engine," *Renewable and Sustainable Energy Reviews* 70, no. 1 (2017): 563–588.

38. S. Vellaiyan and K. S. Amirthagadeswaran, "The Role of Water-in-Diesel Emulsion and Its Additives on Diesel Engine Performance and Emission Levels: A Retrospective Review," *Alexandria Engineering Journal* 55, no. 3 (2016): 2463–2472.

39. M. Ghanbari, L. Mozafari-Vanani, M. Dehghani-Soufi, and A. Jahanbakhshi, "Effect of Alumina Nanoparticles as Additive With Diesel–Biodiesel Blends on Performance and Emission Characteristic of a Six-Cylinder Diesel Engine Using Response Surface Methodology (RSM)," *Energy Conversion and Management: X* 11 (2021): 100091.

40. A. K. Agarwal, A. P. Singh, and V. Kumar, "Particulate Characteristics of Low-Temperature Combustion (PCCI and RCCI) Strategies in Single Cylinder Research Engine for Developing Sustainable and Cleaner Transportation Solution," *Environmental Pollution* 284 (2021): 117375.

41. A. K. Agarwal and M. Krishnamoorthi, "Review of Morphological and Chemical Characteristics of Particulates From Compression Ignition Engines," *International Journal of Engine Research* 24, no. 7 (2023): 2807–2865.

42. D. Singh, D. Sharma, S. L. Soni, et al., "A Comprehensive Review on 1st-Generation Biodiesel Feedstock Palm Oil: Production, Engine Performance, and Exhaust Emissions," *BioEnergy Research* 14, no. 1 (2020): 1–22.

43. R. Senthil and G. A. Vijay, "Review of Physicochemical Properties and Spray Characteristics of Biodiesel," *Environmental Science and Pollution Research* 30, no. 25 (2023): 66494–66513.

44. G. Azhaganathan and A. Bragadeshwaran, "Critical Review on Recent Progress of Ethanol Fuelled Flex-Fuel Engine Characteristics," *International Journal of Energy Research* 46, no. 5 (2022): 5646–5677.

45. K. Nahar, "*Jatropha curcas* L: A Potential 2G Energy Crop to Produce Biofuel in Bangladesh," (2025).

46. M. S. Gad, A. S. El-Shafay, and H. M. Abu Hashish, "Assessment of Diesel Engine Performance, Emissions and Combustion Characteristics Burning Biodiesel Blends From Jatropha Seeds," *Process Safety and Environmental Protection* 147 (2021): 518–526.

47. B. Musthafa and M. A. Asokan, "A Comparative Study of Fuel Filterability, Performance, and Emission Characteristics in CI Engine Fuelled With a Dual Biodiesel Mixture Blended With Conventional Diesel," *Solid Fuel Chemistry* 57, no. S1 (2023): S42–S52.

48. B. R. Varpe, Y. R. Kharde, K. F. Rahman, and A. Khidmatgar, "Effect of Diethyl Ether Additive in Jatropha Biodiesel-Diesel Fuel Blends on the Variable Compression Ratio Diesel Engine Performance and Emissions

Characteristics at Different Loads and Compression Ratios," *Heat Transfer* 49, no. 8 (2020): 4427–4447.

49. M. A. Fayad, S. I. Ibrahim, S. H. Omran, et al., "Experimental Effect of CuO_2 Nanoparticles Into the RME and EGR Rates on NO_X and Morphological Characteristics of Soot Nanoparticles," *Fuel* 331 (2023): 125549.

50. S. K. Dash, D. Dash, P. K. Das, et al., "Investigation on the Adjusting Compression Ratio and Injection Timing for a DI Diesel Engine Fueled With Policy-Recommended B20 Fuel," *Discover Applied Sciences* 6, no. 8 (2024): 1–18.

51. O. A. Qamar, F. Jamil, M. Hussain, et al., "Advances in Synthesis of TiO_2 Nanoparticles and Their Application to Biodiesel Production: A Review," *Chemical Engineering Journal* 460 (2023): 141734.

52. G. Zhu, C. Wen, T. Liu, et al., "Combustion and Co-Combustion of Biochar: Combustion Performance and Pollutant Emissions," *Applied Energy* 376 (2024): 124292.

53. C. Jit Sarma, P. Sharma, B. J. Bora, et al., "Improving the Combustion and Emission Performance of a Diesel Engine Powered With Mahua Biodiesel and TiO_2 Nanoparticles Additive," *Alexandria Engineering Journal* 72 (2023): 387–398.

54. R. Küçükosman, A. A. Yontar, and K. Ocakoglu, "Nanoparticle Additive Fuels: Atomization, Combustion and Fuel Characteristics," *Journal of Analytical and Applied Pyrolysis* 165 (2022): 105575.

55. F. Sharifianjazi, A. H. Esmaeilkhanian, N. Karimi, et al., "A Review of Combustion Properties, Performance, and Emission Characteristics of Diesel Engine Fueled With Al_2O_3 Nanoparticle-Containing Biodiesel," *Clean Technologies and Environmental Policy* 26, no. 11 (2024): 3715–3737.

56. J. Lv, S. Wang, and B. Meng, "The Effects of Nano-Additives Added to Diesel-Biodiesel Fuel Blends on Combustion and Emission Characteristics of Diesel Engine: A Review," *Energies* 15, no. 3 (2022): 1032.

57. L. Razzaq, M. M. Abbas, A. Waseem, et al., "Influence of Varying Concentrations of TiO_2 Nanoparticles and Engine Speed on the Performance and Emissions of Diesel Engine Operated on Waste Cooking Oil Biodiesel Blends Using Response Surface Methodology," *Heliyon* 9, no. 7 (2023): e17758.

58. S. M. A. Ibrahim, K. A. Abed, M. S. Gad, and H. M. A. Hashish, "Performance and Emissions of a Diesel Engine Burning Blends of Jatropha and Waste Cooking Oil Biodiesel," *Proceedings of the Institution of Mechanical Engineers, Part C: Journal of Mechanical Engineering Science* 238, no. 4 (2024): 1157–1169.

59. M. R. Rahim, N. Othman, A. S. Araibi, A. P. Trisasongko, M. S. Abdul Malik, and M. Said, "Mitigation of Nox and Co Emissions From Liquid Fuel Burner Firing Jatropha Biodiesel Blends," *Jurnal Teknologi (Sciences & Engineering)* 87, no. 3 (2025): 465–473.

60. A. S. El-Shafay, M. A. Mujtaba, F. Riaz, and M. S. Gad, "Investigating the Role of Hybrid Binary Feedstocks (Waste Cooking Oil, Palm Oil, and Jatropha Oil Blends) in Biodiesel Production: Engine Performance, Emissions, and Combustion Characteristics," *Case Studies in Thermal Engineering* 73 (2025): 106688.

61. K. V. Yatish, H. R. Chandan, S. M. Shankar, and B. R. Omkaresh, "Advancements in Reactor Technologies for Scalable and Sustainable Biodiesel Production," *ChemBioEng Reviews* 12, no. 2 (2025): e70001.